"SEGMENTATION OF ECHOCARDIOGRAPHIC IMAGES FOR MITRAL REGURGITATION EVALUATION"

A ProjectReport

Submittedin partialfulfillment of

therequirementsforthe award of the degree

of

MASTER OFTECHNOLOGY

in

ELECTRICAL ENGINEERING
(WithSpecializationinInstrumentation and Signal Processing)

Submittedby

SANTHIYA T (EnrollmentNo: 16528008)

Under the guidanceof

Dr. R. S. ANAND

DEPTT. OFELECTRICAL ENGINEERING
INDIANINSTITUTE OFTECHNOLOGYROORKEE
ROORKEE-247667(INDIA)
September 2018

CANDIDATE'S DECLARATION

I hereby declare that this thesis report entitled **Segmentation of Echocardiographic images for Mitral Regurgitation Evaluation,** submitted to the Department of Electrical Engineering, Indian Institute of Technology, Roorkee, India; in partial fulfilment of the requirements for the award of the Degree of Master of Technology in Electrical Engineering with specialization in Instrumentation and Signal processing is an authentic record of the work carried out by me during the period June 2017 to September 2018, under the supervision of Dr. R. S. Anand, Department of Electrical Engineering, Indian Institute of Technology, Roorkee. The matter presented in this thesis report has not been submitted by me for the award of any other degree of this institute or any other institutes.

Date: Santhiya T

Place: Roorkee Enrol. No: 16528008

CERTIFICATE

This is to certify that the above statement made by the candidate is true to the best of my knowledge and belief.

Dr. R. S. Anand

Professor

Department of Electrical Engineering

IIT Roorkee.

ACKNOWLEDGEMENT

I am highly indebted to Dr. R. S. Anand for providing me his valuable time and constant support in completing this project. I would like to take this opportunity to express my profound gratitude to him for his guidance as well as his personal interest in my project. His immense knowledge in the field of Biomedical Signal Processing and the belief he had in me helped me to achieve the objective of this project. I am grateful to my institution, Professors of Electrical Engineering Department, my colleagues, my friends and the research scholars for providing me constant encouragement and support, which helped me to renew my spirit and refocus my attention in carrying out this work.

Date: 25/09/2018 SANTHIYA T

Place: Roorkee MTech (Instrumentation and Signal Processing)

ABSTRACT

The color Doppler echocardiography is used to detect the blood flow patterns, direction, and velocity in case of any abnormality such as valvular regurgitation and stenosis. In present days, the clinicians analyse the severity of mitral regurgitation (MR) by manually ascertaining regurgitant jet area with the assistance of cursor in the echocardiographic images. This paper focuses on automatic segmentation of the color mosaic pattern from echocardiographic images to determine the regurgitant jet area and finding its value in numerical terms. The evaluated jet area is then associated with the level of the severity of MR in particular mild, moderate and severe. For segmentation of echocardiographic images, the proposed strategy incorporates different segmentation algorithms like color space model, thresholding, and morphological operators. A total of 75 images have been examined taken from 25 patients suffering from MR. The severity of MR has been resolved in view of the regurgitant jet area got from the proposed technique and are compared with the manual method of assessment of MR. The algorithm developed is capable of removing the imitative areas during the process of segmentation. The regurgitant jet area acquired from the proposed strategy fulfils the clinical outcomes in the fast assessment of severity of MR.

CONTENTS

Title **Page.no**

LIST OF FIGURES

CHAPTER 1

INTRODUCTION

Medical imaging gives a viable and non – intrusive representation of life structures of human body. The patterns displayed by the natural tissues in the images have been used with the end goal of medicinal diagnosis, as various tissue neurotic conditions create diverse image patterns. The fast improvement and expansion of medical imaging innovation has changed the medicinal field and the part of restorative imaging has extended past the basic representation and investigation of anatomical structure.

The most difficult issue in medical imaging is the examination of images got through X-ray, Computed Tomography (CT), Magnetic Resonance Imaging (MRI), Positron Emission Tomography (PET), Ultrasound and different modalities. Investigation of restorative images includes extricating valuable data of the anatomical structures. These imaging innovations give excellent perspectives of internal anatomy where prepared radiologists evaluate and examine the installed structures. Anyway manual investigation of restorative images is a tedious procedure other than being defenceless to human mistakes. To defeat the issues related with the manual investigation, the computer based approaches are used for understanding the medical images [2].

1.1 ULTRASOUND IMAGING

Diagnostic ultrasound, otherwise called restorative sonography or ultrasonography, utilizes high recurrence sound waves to make images. The ultrasound machine sends sound waves into the body and can change over the returning sound echoes into an image. Ultrasound technology can likewise deliver discernible hints of blood stream, enabling medicinal experts to utilize the two sounds and visuals to evaluate a patient's wellbeing.

Ultrasound is frequently used to assess:

- Pregnancy
- Abnormalities in the heart and veins
- Organs in the pelvis and belly
- Symptoms of agony, swelling and disease

1.1.1 The Ultrasound Imaging Process

The imaging Process in ultrasonic imaging is like the radar guideline. The tissue is presented to sound waves of settled recurrence. In this manner, the reflections that are produced amid the spread of sound waves are enlisted as a component of time.

The exact time difference between the transmission and reception of pulses reveal the intricate structures present in tissues. And the pulses received by this way are used in the formation of an image. Formation of an image in ultrasound is shown in the fig.1.1.

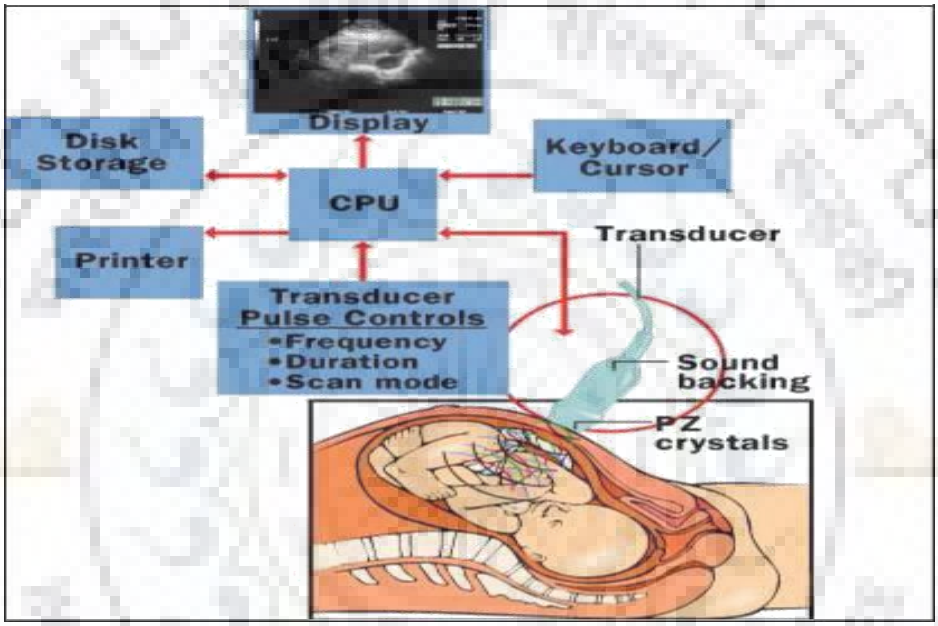

Figure 1.1 Image formation in ultrasound.

The transducer that is used by the clinicians for imaging the body has dual property. It acts as both transmitter and receiver. While transmitting the transducer produces sound waves by converting the electrical signals to mechanical vibrations. The turnaround marvel happens in the receiving procedure, where the received ultrasound waves created at the interfaces, are changed over into electrical signs[4]. This chips away at piezoelectric impact. The materials showing piezoelectric property are utilized for such reason. In restorative ultrasound gear, lead zirconate titanate is most broadly utilized as a transducing material.

Piezoelectric materials contain sub-atomic dipoles, where positive and negative charges are isolated. Applying an electric pulse over a piezoelectric crystal makes those dipoles change its orientation, bringing about difference in the material thickness[9]. Then again, if mechanical power is connected to the crystal, the sub-atomic dipoles change their orientation, which adjusts the electric field and results in potential distinction over the crystal.

This property makes the piezoelectric crystal reasonable to deliver sound waves and a microphone is utilized to record the returning reflections.

The sound waves get reflected at the interface of tissues with different acoustic impedances. The acoustic impedance Z of a material is portrayed as the consequence of its thickness ρ and speed of the sound v (i.e.)

$$Z=\rho v. \quad (1.1)$$

The sound package is known to reflect basically at the tissue-air interface. Hence if there is an air ascend en route of the sound wave, a dull spot is found in the ultrasound check. The reducing of the ultrasound essentialness observable all around is high and along these lines no reflection can be received when the ultrasound columns multiply through the air. In this way authentic coupling must be made between the transducer and the tissue interface. Therefore, clinicians put some coupling gel on the skin surface where the transducer is to be put[8]. A modification in tissue makes, and from this time forward a sudden change in acoustic impedance, causes specular impression of the sound package. The part of these reflections that adds to the bearing where the event sound package starts from is known as the back scattered flag.

1.2 MODES OF ULTRASOUND

The ultrasound imaging used in clinical areas can be classified into different modes such as A-mode, B-mode, M-Mode, Doppler-Mode, Duplex-Mode, 3D-Mode and the recent advanced mode being the 4D-Mode.These different types of modes of ultrasound imaging are used during each of the echocardiographic examination. One type of mode creates a complementary finding from the other modes of the examination and hence different modes are performed simultaneously.

1.2.1 A-Mode

A-Mode in ultrasound imaging stands for Amplitude Mode. It is the simplest of all the modes used for ultrasound imaging. A single transducer probe is used here, with echoes plotted with the function of depth in the body. The amplitude of the echoes reflected is visualized with the help of oscilloscope [6]. The waveform has spikes of different amplitude. This method is used to measure distances of the body organs and also in the determination of the size of organs. A-Mode image obtained from the scanning of optical nerve is shown in the fig.1.2.

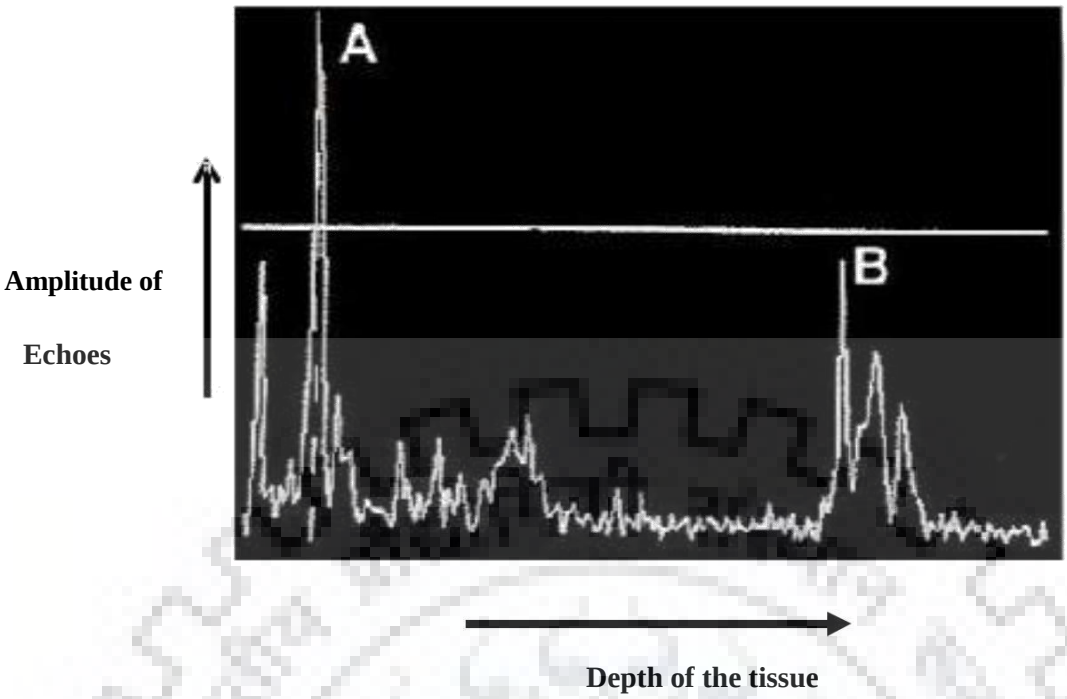

Figure 1.2 A-Mode image obtained from the scanning of optical nerve [1].

1.2.2 B-Mode

B-Mode or Brightness Mode is the most common form of ultrasound imaging. It displays 2D map of the data. In B-Mode there is no presence of vertical spikes instead it produces various points of brightness, which depends on amplitude or intensity of the echo. The field of view is the portions of organs or tissues intersected by scanning plane. The horizontal position of each bright dot represents location of the receiving transducer element and the vertical position of bright dot represents the echo intensity or amplitude[6]. B-Mode will display image of large and bright dots representing strong and weak echoes respectively.

The piezoelectric transducer used for ultrasound imaging can be fabricated in number of ways. The major two types are sector type and rectangular or trapezoid type. The rectangular or trapezoid type is used for producing the images of superficial or vascular tissues. The sector type is used to obtain the image of abdominal tissues. Based on the number of the elements of the transducer used, B-Mode images can be classified as linear and phased array[6]. In case of phased array all the elements are used simultaneously and in case of linear array only a subset of total array elements are used. Linear array saves the electronic hardware used but the time taken to image the field of view is very high. Linear array and phased array probes are shown in fig.1.3.

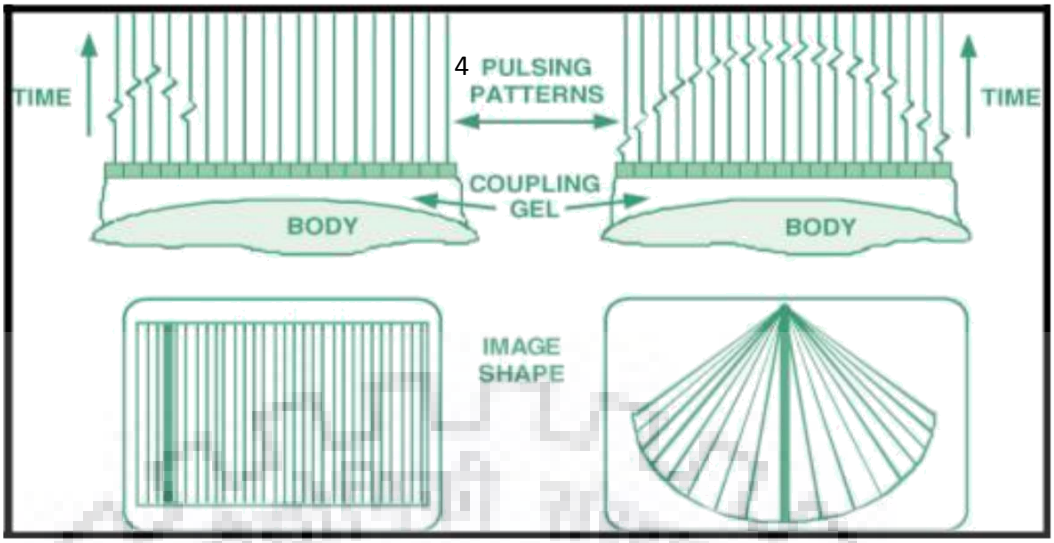

Figure 1.3 Linear array and phased array probes [2].

In case of B-Mode, if the probe movement is performed manually, then it is called as compound and static B-scanner and if the probe movement is performed automatically then it is called as real time scanner. Real time data can be represented by repeatedly activating the crystals many times.

Uses of B-Mode Ultrasound in clinical area:

- Abdominal Imaging
- Cardiology
- Obstetrics
- Peripheral Vasculature.

1.2.3 M-Mode

M-Mode remains for Motion Mode. It is a fast succession of A-mode that takes images back to back on screen that empowers specialists to see and measure scope of movement, as the organ limits that deliver reflections move with respect to the test. M-Mode ultrasound has been put to specific use in considering heart movement [3]. In M-Mode ultrasound the transducer is kept stationary and the echoes from moving reflector are considered after some time. It has great fleeting goals; henceforth it is utilized in identifying quick developments. Higher examining recurrence up to 1000pulses/sec is helpful in evaluating rates and movement. Movements of Mitral leaflets over time are shown in fig.1.4.

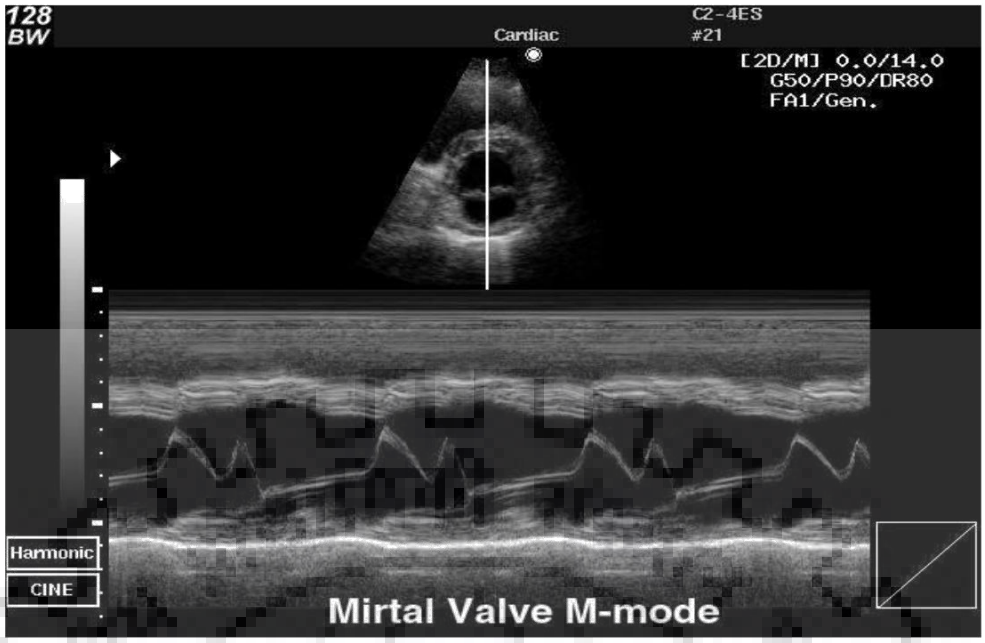

Figure.1.4 Movements of Mitral leaflets over time [3].

Uses of M-Mode Ultrasound in clinical area:

- Adult cardiac imaging
- Fetal cardiac imaging

1.2.4 Color Doppler Mode

It gives 2D image superimposed by color indicating the direction and velocity of blood. This mode uses low frequency ultrasound image for deriving the image hence its quality seems deteriorated. Schematic diagram of color Doppler is shown in fig.1.5.

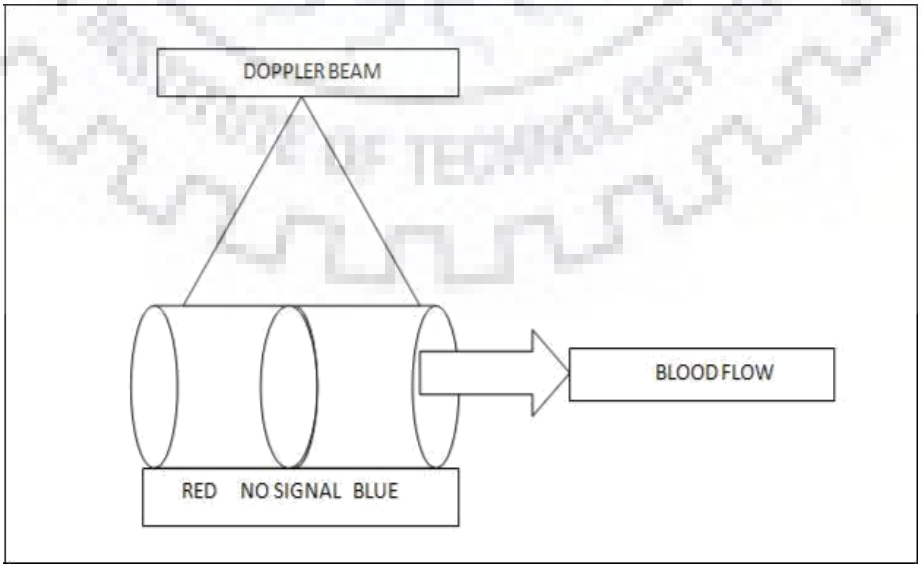

Figure 1.5 Schematic diagram of color Doppler [4].

By tradition, blood streaming far from the test is portrayed in blue and blood streaming towards the test in red. Blood streaming opposite to the examining plane will seem dark. Regions of tempestuous stream might be portrayed in green or white. Mitral valve Regurgitation in color Doppler mode is shown in fig.1.6.

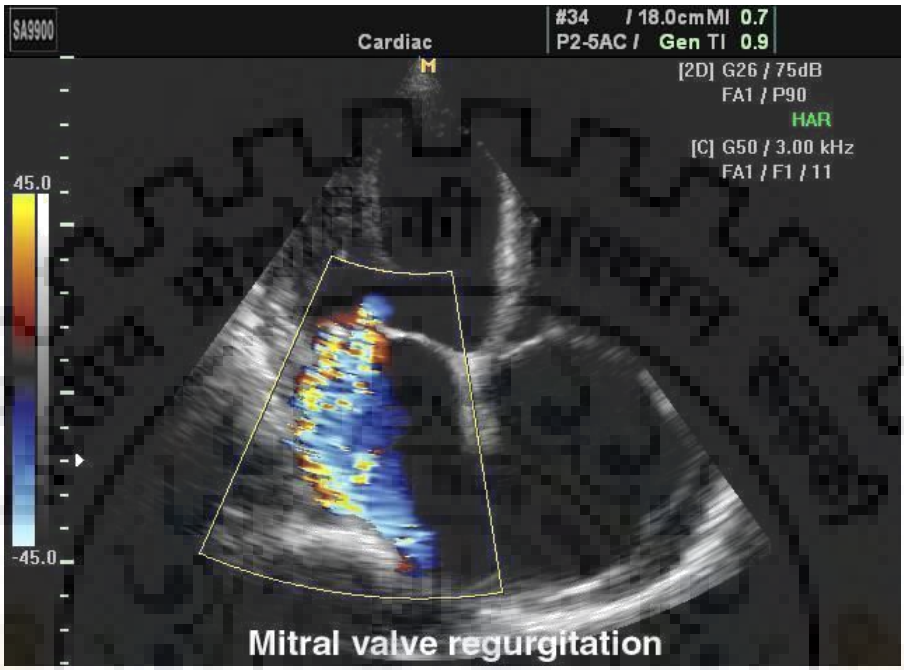

Figure 1.6 Mitral valve Regurgitation in color Doppler mode [3].

1.2.5 Pulse Wave Doppler Mode (PWD)

The Doppler signal gives the velocity and direction of the blood flow. The ultrasound signal is transmitted using a transducer containing the piezoelectric crystal. Hence it helps us to exactly identify the region from which the velocity signal arises.

From PWD, the user can also examine the type of flow whether it's laminar or turbulent. The laminar flow appears as a thick waveform with dark region inside. This is because of the presence of large count of RBC's moving at similar speed. This phenomenon is termed as phantom expanding.

Thus pulse wave Doppler serves for dual use it is not only used for determining the velocity and direction of blood stream but it is also used to determine the type of flow be it laminar or turbulent. PWD through left ventricular outflow tract is shown in fig.1.7.

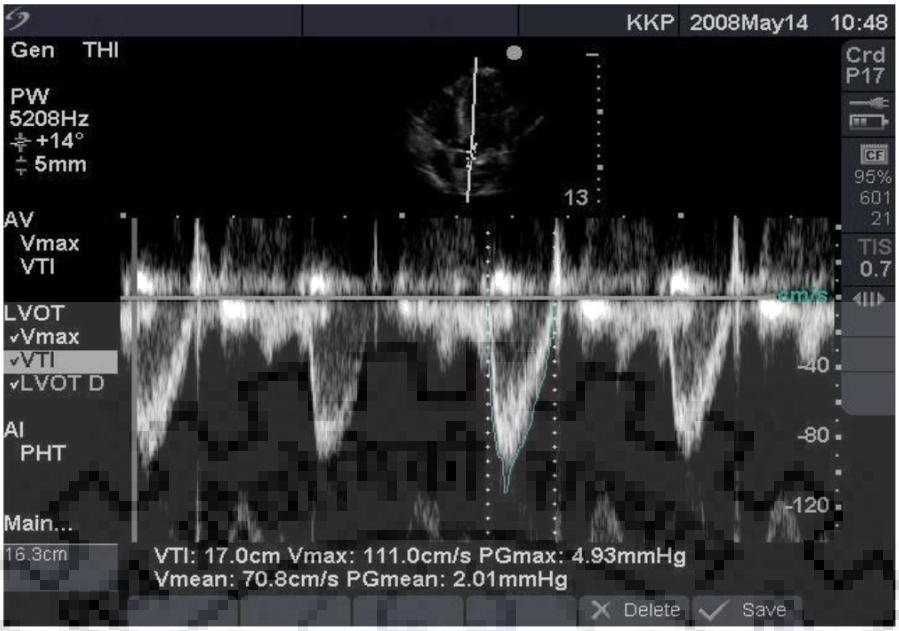

Figure 1.7 PWD through left ventricular outflow tract [3].

1.2.6 Continuous Wave Doppler Mode (CWD)

Two transducers are used here, one is continuously transmitting and the other one is continuously receiving along a line on the 2D image. CWD is used for determining higher velocities but it fails to give the exact location of origin of the signal. Hence CWD is preferred in applications where high velocities of the blood stream have to be measured accurately. CWD of Mitral Regurgitation jet is shown in fig.1.9.

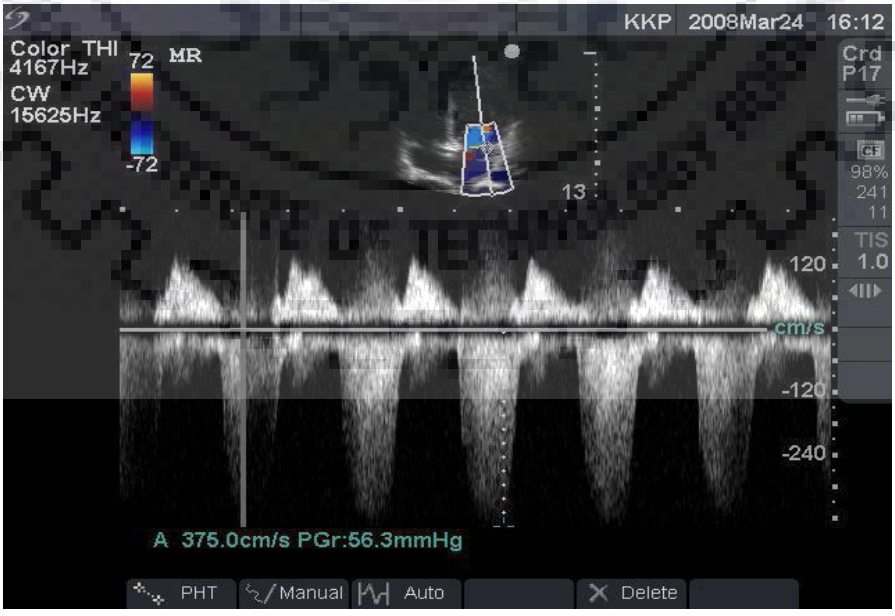

Figure 1.9 CWD of Mitral Regurgitation jet [3]

1.2.7 Tissue Doppler Mode

This mode gives a waveform similar to PWD; the key difference is that, it is used to measure the speed of the tissue undergoing development. The rate of tissue development is much lower than the speed of blood flow. Here the cursor is positioned on the tissue, for which the development rate has to be monitored. Tissue Doppler through Mitral annulus is shown in fig.1.10.

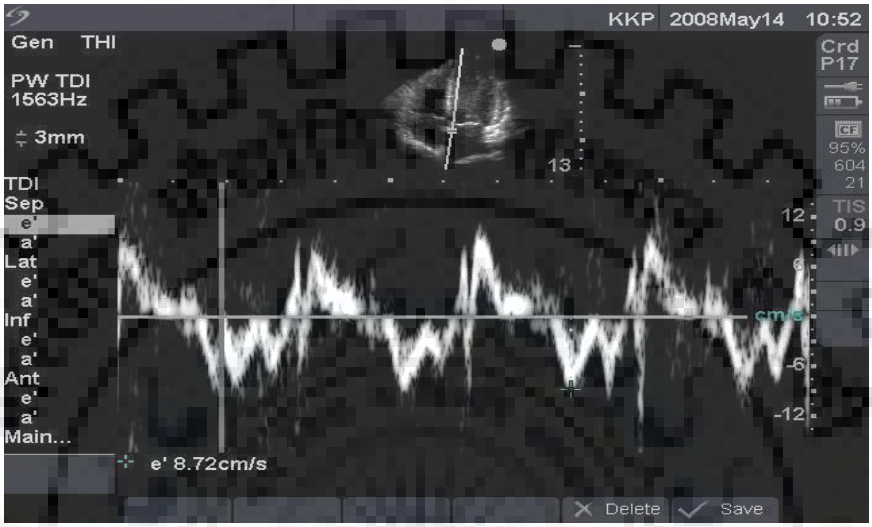

Figure 1.10 Tissue Doppler through Mitral annulus [3].

1.2.8 DUPLEX Mode

Duplex Mode uses traditional ultrasound and Doppler Ultrasound. It is used in the diagnosis of Venous and Arterial disease [8]. Traditional Ultrasound gives the static image of the affected veins. Doppler ultrasound gives information about the blood flow through the veins. Duplex Mode overlaps the images obtained by both traditional ultrasound and Doppler Ultrasound and facilitates interpretation. Duplex scan of Peripheral Artery is shown in the fig.1.11.

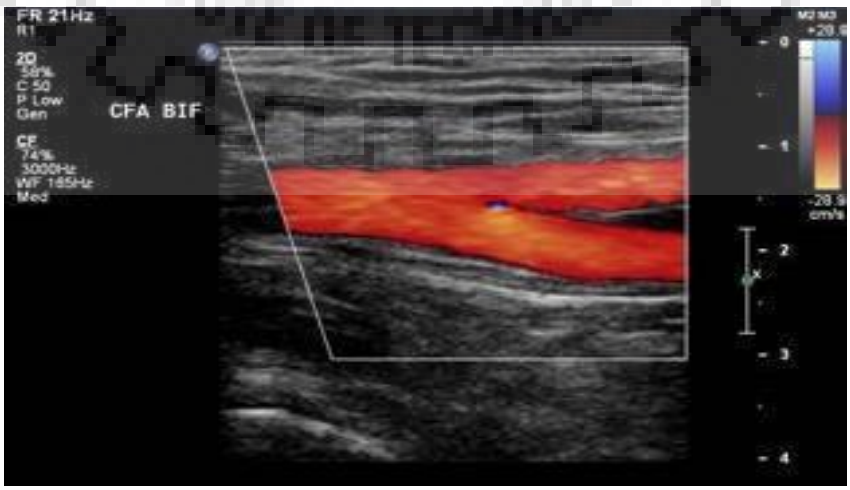

Figure 1.11 Duplex scan of Peripheral Artery [4].

1.2.9 Tissue Harmonic Imaging Mode

Conventional ultrasound transmits and receives signal of specific frequency. But in case of Tissue Harmonic Imaging the received signal contains the harmonic frequency along with the fundamental frequency. The Harmonic frequency received is twice that of the fundamental frequency. The harmonic frequency is generated in two different ways,

- By injecting contrast agents at the specific location
- Due to the interaction of the ultrasound with the tissues.

1.2.10 3D MODE

3D ultrasound is a technique for checking the internals of a man and producing a 3D picture. While most are usually connected with obstetric ultrasonography and following fetal development all through pregnancy, it has likewise given progressive strategies in other therapeutic zones [3]. 3D Mode includes procurement of volume information by progressive gathering of somewhat unique 2D pictures. These 2D pictures are coordinated by fast PC programming.

Volume information can be procured by three procedures;

- Free hand development of test.
- Mechanical sensors incorporated with the test.
- Matrix exhibit of sensors that consolidates arrangement of 2D outlines in progression.

Figure 1.12 3D Mode Displaying organ or Skin surface [9].

Figure 1.13 3D Mode Displaying fetal Skeleton [9].

1.2.11 4D MODE

4D Mode ultrasound is a 3D ultrasound in live movement and it the most developed method of ultrasound imaging. In the 4D ultrasound, the fourth measurement is time. 3D Mode includes development and makes the most practical portrayal of all. It utilizes 2D ultrasound which quickly gains 20-30 volumes or a framework exhibit 3D transducer [4]. 4D Ultrasound is most generally utilized for watching the movement of fetal heart valves or blood stream in their vessels.

1.3 Comparison of Ultrasound Imaging Modes

S.NO	MODES	MERITS	DEMERITS
1.	A - MODE	• Depth of an organ. • Organ's dimensions.	• Scans along a line (1D).
2.	B - MODE	• 2D structure of the tissue can be visualized through this.	• Rapid movements cannot be determined.
3.	M - MODE	• Good temporal resolution	• Very high sampling rates are required.
4.	DOPPLER MODE	• To measure Relative velocities. • Information about the Direction of flow	• Reduced frame rate also reduces temporal resolution. • Ultrasound beam should be held parallel to the blood flow.
5.	PWD - MODE	• It depicts the velocity of flow. • Nature of flow-laminar or turbulent.	• Inability to measure high velocities accurately.
6.	CWD -MODE	• Good resolution can be achieved for high velocities.	• Location of the signal cannot be found.
7.	DUPLEX MODE	• Diagnosis of venous and arterial disease.	• More time consuming.
8.	TISSUE DOPPLER	• Measures velocities of tissue movement	• Only suitable for lower velocity measurement.
9.	THI	• The properties of Harmonic signals improve the spatial and contrast resolution.	• Has poor lateral resolution as the benefits of THI are more apparent in the centre portion of the ultrasound image.
10.	3D MODE	• More complete image of a developing fetus.	• Shows static image of the internals of the person.
11.	4D MODE	• Visualizing heart wall motion in cardiology.(Real time)	• Can lead to false positives. Enhance the noise and disruptions.

1.4 HEART FUNCTION

The heart is a strong organ about the measure of a clench hand, found simply behind and somewhat left of the breastbone [4]. The cardiovascular system acts as the network of veins and arteries through which the pumping of blood takes place through the heart. Function of Heart is shown in the fig.1.14.

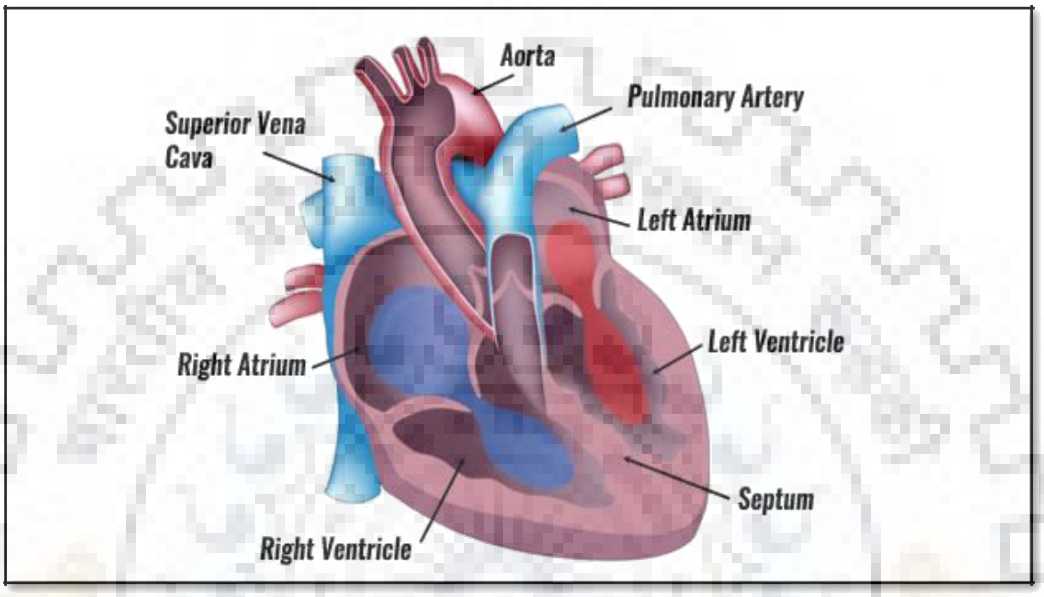

Figure 1.14 Function of Heart [4].

The heart has four chambers:

- The right atrium pumps blood to the right ventricle by receiving it from the veins.
- The right ventricle in turn pumps it to the lungs.
- The left atrium pumps the oxygenated blood to the left ventricle by receiving it from the lungs.
- Then the oxygen rich blood is supplied to the rest of the body through left ventricle.

1.5 HEART VALVES

Human heart valves are momentous structures. The thin layers that are attached to the heart controls the blood flow by opening and closing, thus causing heartbeat sound. T Each beat is an astounding presentation of quality and adaptability. Various valves of the heart are shown in fig.1.15.

The heart has 4 valves:

- The mitral and tricuspid valve regulates the blood flow into the ventricles from atria.
- The pulmonary and aortic valve regulates the blood flow out of ventricles.

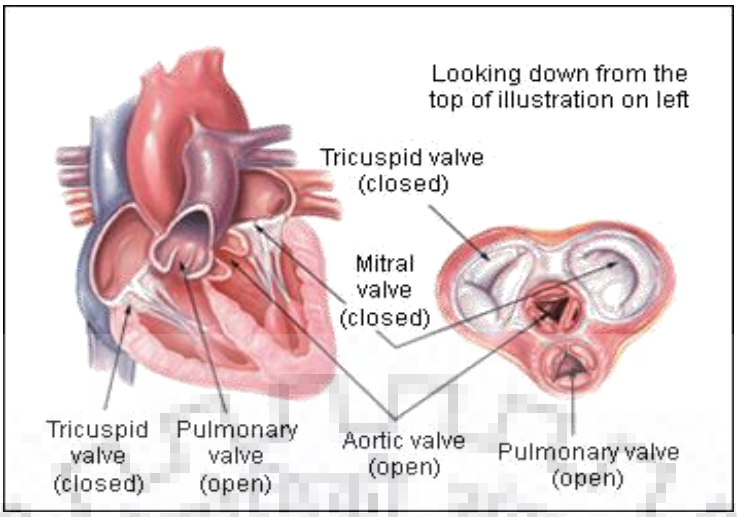

Figure 1.15 Representation of various valves of the Heart [4].

A typical, heart valve limits any block and enables blood to stream easily and uninhibitedly one way. It closes totally and rapidly, not enabling any blood to stream back through the valve.

1.6 HEART DISEASE

VHD is caused due to the defect in one of the four heart valves: the aortic, mitral, pulmonary or tricuspid. Mitral and Aortic valves are most commonly affected valves due to the valvular heart disease. VHD can cause insufficiency (regurgitation), stenosis or both in some of the patients. If the valves are unable to open completely it is known as stenosis and if the valves are unable to close completely thereby allowing backflow of blood is known as regurgitation.

Mitral Regurgitation (MR) is a common heart valve disorder with no symptoms in most of the patients and hence in present days clinicians are using echocardiographic images to diagnose it. In echocardiography, color Doppler images help in accurate evaluation of mitral regurgitation. In present days clinicians determine the severity of MR by manually calculating the regurgitant jet area from the echocardiographic images. But it is not reliable as the accuracy of determination of the VHD is highly dependent on the person operating the ultrasound machine. The diagnosis of the severity of the VHD may vary from the actual condition of the patient leading to mistreatment. Hence there is a need for automatic evaluation of Mitral Regurgitation.

The mitral regurgitation in the echocardiographic images can be viewed in three views: apical two chamber (A2C), apical four chamber (A4C) and parasternal long axis (PLAX). The A2C view depicts the anterior and inferior walls of the left ventricle.

The A4C view shows all the four chambers of the heart. The A4C view is considered to be the best view by the clinicians to study inflow and to visualize the apex of the left ventricle. The PLAX view helps in the measurement of the size of both left and right ventricle and also for the interpretation of the VHD [31]. In the present days all the three views of the patients are used by the clinicians for diagnosing the severity of MR.

Lots of work has been done in the literature regarding segmentation of medical images. Color acts as one of the fundamental properties of objects and has been used as important cue in several object segmentation frameworks [27]. The colors present in the Doppler images of echocardiography helps to manipulate images for segmentation of the color mosaic pattern by using different color space models. Various thresholding techniques for image segmentation like Histogram dependent thresholding, adaptive thresholding techniques are discussed in [32]. Automatic segmentation of Ultrasound images using Morphological operators is proposed in [18].

1.7 LITERATURE REVIEW

Judith et al. [17] proposed a technique for automatic segmentation of ultrasound images using Morphological operators. Using this technique he has performed fetul femur length measurement using B mode images. Cheng et al. [18] introduced a method for the boundary detection of the left ventricle using watershed transform and morphological operators. Wolfe et al. [19] performed a study for tracing the endocardial and epicardial boundaries of the heart in phantom image using Haralick's method of edge detection.

Ventricular contour detection in ultrasound images was done by thresholding based edge detection method is demonstrated by Lamberti et al. [20]. Sheng et al. [21] advocated in their study that segmentation of left ventricle can be done by shape based snake model combined with generalized Hough Transform. Mikic et al. [22] proposed a technique for tracing the boundaries of Mitral valve leaflets, Aortic valve and Left ventricle using active contour guided optical flow estimates. Boonchieng et al. [23] performed a study to generate a contour line of endocardium border using sobel compass gradient mass edge detection method. Baldevbhai et al. [24] has reviewed and made comparison between some of the basic methods of segmentation like graph image based segmentation, medical image based segmentation and color image based segmentation. Paschos et al. [25] has presented a methodology that uses Gabor filter to measure specific sizes and orientations within the color texture and the experimental results are obtained for various color texture images.

Khattab et al. [26] has presented a comparative study to evaluate the performance of color image segmentation in different color spaces using GrabCut technique. Automation of the GrabCut method has been proposed to avoid the user's interaction for initialization. Kaur et al. [27] has proposed a color image segmentation algorithm for segmentation of images based on the colors present in it. Here the original RGB image is converted into HSV color space and is used for segmentation. Zhang et al. [28] has described about a classifier design and has validated its performance for assessment of mitral regurgitation (MR) quantitatively. 2D echocardiographic images were used for the assessment of MR. Grimes et al. [29] has applied dimensional analysis for the evaluation of the function of left ventricle (LV) in the presence of MR. In the presence and absence of MR a computer model was used to stimulate ventricular hemodynamics. Khayum et al. [30] has presented anisotropic diffusion method for quantification of MR, in addition to that he has also proximal flow convergence method for flow field measurements. Kirsner et al. [31] has quantitatively determined the severity of MR using automated analysis of Doppler power spectrographs. He has used mitral regurgitant fraction (MRF) as a quantitative measure for determining the severity of MR. Hergum et al. [32] has developed a 3D ultrasound Doppler method to determine the geometry and cross-sectional area of the regurgitant jet at vena contracta. Computer simulations have been used to verify and implement this method. Song et al. [33] has used Support Vector Machine (SVM) for analysing the function of mitral complex geometry from 3D Echocardiography. He has used SVM as a classifier to diagnose congenital mitral regurgitation.

Deserranno et al. [34] has developed a model based on normalized centreline velocity distribution for quantification of mitral regurgitation automatically. He has used computational fluid dynamics for accurate evaluation of MR. Simone et al. [35] has developed a method for reconstruction of color Doppler flow signals in 3D and for segmentation of regurgitant jet. He has given a quantitative measure of the volume of the regurgitant jet area. Karlsson et al. [36] has developed a computer simulation for improved assessment of mitral regurgitation by studying the non-planar geometry and the proximal velocity field for non-stationary flow.

CHAPTER 2

SEGMENTATION OF ECHOCARDIOGRAPHIC IMAGES

2.1 SEGMENTATION

A formal definition of image segmentation is as per the following [10]: If F is the arrangement of all pixels and P() consistency (homogeneity) predicate characterized on gatherings of associated pixels, at that point division is a dividing of the set F into an arrangement of associated subsets or districts *(S_1, S_2, ...Sn)* to such an extent that $\bigcup_{i=1}^{n} S_i = F$ with $i \cap S_j = \Phi, (i \neq j)$. The consistency predicate *$P(S_i)$ = true* for all regions *(S_i and Si $\cap S_j$ = false*, when *$(i \neq j)$* and S_i is neighbouring S_j.

2.2 PROPOSED METHOD FOR SEGMENTATION OF MR

To accomplish the segmentation of color Doppler images of MR the execution steps of the proposed technique are portrayed in Figure.2.1. The execution steps of the proposed technique are according to the following:

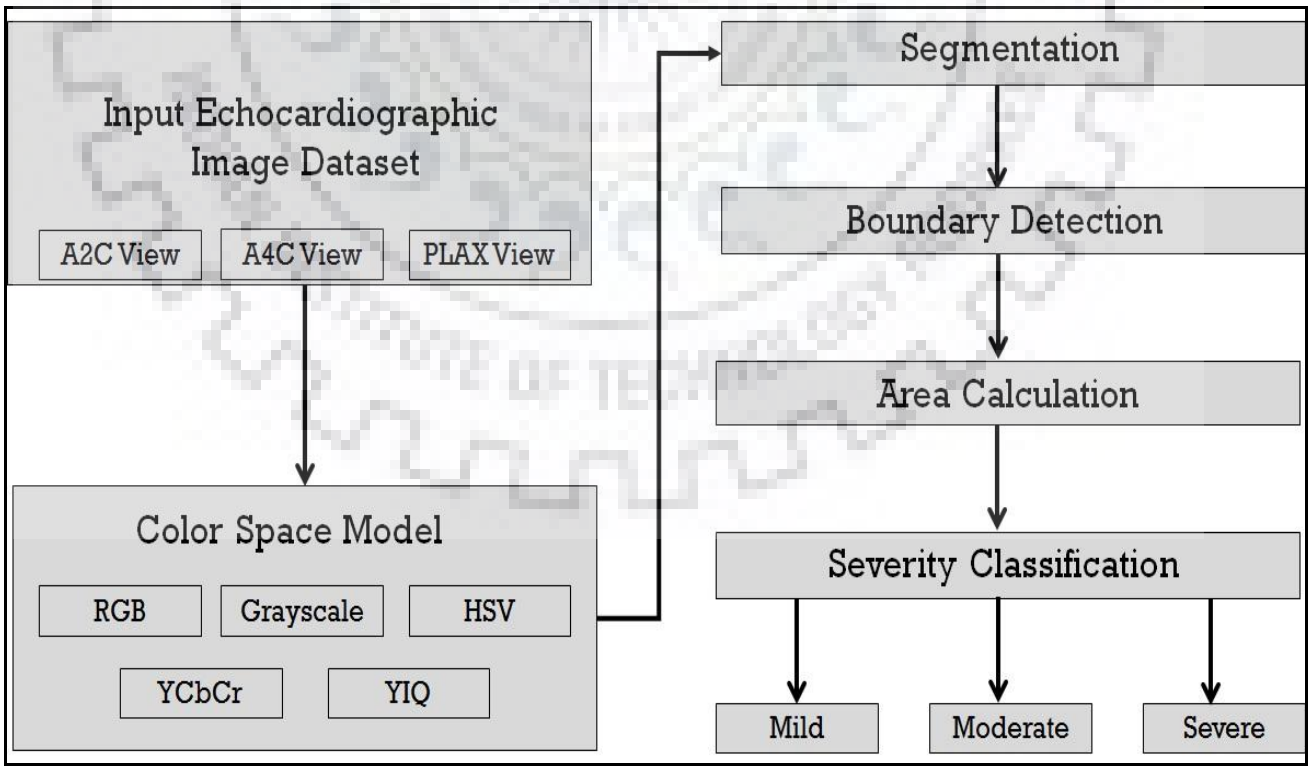

Figure 2.1 Steps of the proposed algorithm for segmentation of MR

2.2.1 Color space model

Selection of color space model for segmentation depends on the application of interest. In the literature different color spaces has been proposed, each with its own properties, advantages and drawbacks. In this work four different color spaces namely RGB, HSV, YCbCr, YIQ are used. RGB Color space is the simplest and most commonly used color space for representation of digital image. The RGB color space is represented by red (R), green (G), and blue (B) chromaticities. The image represented in RGB color space has additive combination of these primary colors.

The HSV color space is represented by Hue (H), Saturation (S) and Value (V). The position of the color in a 360 degree spectrum is described by Hue. The pureness of the color is indicated by Saturation, it measures the difference between the color and a grayscale value of equal intensity. The third channel value measures the brightness of the color [10]. In YCbCr color space model, the chrominance information is stored as two different components (Cb and Cr) and the luminance information is stored only as a single component (Y). YCbCr signals are created from the corresponding gamma adjusted RGB source using three different constants K_R, K_G and K_B as follows,

$$Y' = K_R R' + K_G G' + K_B B' \tag{2.1}$$

$$P_B = {}^1\!/_2 \cdot \frac{B' - Y'}{1 - K_B} \tag{2.2}$$

$$P_R = {}^1\!/_2 \cdot \frac{R' - Y'}{1 - K_R} \tag{2.3}$$

Here, the prime ‘symbol mean gamma correction is used and R’, G’ and B’ has values nominally in the range of 0 to 1.

YIQ color space is defined by the National Television Systems Committee (NTSC) is used in television in United States. The major advantage of this color space is that gray scale information is separated from the color data so that same signal can be used for both color and black and white sets.

Upon conversion of the Input Image into the above mentioned color space models it was observed that the I component of the YIQ color space provided better results for the segmentation of mosaic pattern from the echocardiographic image. In YIQ color space, since the gray scale information is isolated from the color and black and white sets most of the structures present outside the jet area depicted in the color Doppler image can be easily removed though further processing.

2.2.2 Negative Transformation

Negative Transformation is used to obtain the negative of an image having gray level in the range of *[0, L – 1]* and is expressed as in eq.1

$$s = L - 1 - r \tag{2.4}$$

For enhancing the white or gray portions present in the dark regions of the chrominance (I) component of the NTSC color space, negative transformation is performed. Negative transform basically reverses the intensity levels and thus depicts the negative of the image. Hence the chrominance (I) component of the input echocardiographic image in NTSC color space model is negative transformed to extract the white or gray patterns embedded in the dark regions of the mosaic pattern.

2.2.3 Thresholding

Thresholding is used to convert the gray level image obtained as the result of negative transformation into a binary image with only two regions. One region is inside the regurgitant jet area and the other region is outside the regurgitant jet area. In general thresholding may be viewed as an operation that involves tests again a function T of the form

$$T = T[x, y, p(x, y), f(x, y)] \tag{2.5}$$

Where *p(x, y)* denotes some local property of the point *(x, y)* and *f(x, y)* denotes the gray level of point *(x, y)*. Hence the thresholding operation is defined as follows:

$$g(x,y) = \begin{cases} 1, & if\ f(x,y) > T \\ 0, & if\ f(x,y) \leq T \end{cases} \tag{2.6}$$

Where, $f(x, y) > T$ denotes the pixel inside the regurgitant jet area and $f(x, y) \leq T$ denotes the pixel value outside the regurgitant jet area. And here the threshold used is global threshold as the threshold T depends on only the gray level values of the image *f(x, y)*. Thus at the end of thresholding an image with only two regions is obtained, one inside the jet area and the other outside the jet area.

2.2.4 Morphological Operators

Upon successful conversion of the gray level image into a binary image morphological operators are used to remove the discontinuities to get the regurgitant jet area. Here morphological operators like Dilation and erosion are used to get the desired mosaic pattern.

Dilation is used for expanding the shapes present in the input image by using appropriate structuring element depending on the application. Structuring element acts as a mask that helps in defining the arbitrary structures. The dilation of an image I by a structuring element H is defined as

$$I \oplus H = \bigcup_{p \in I} H_p \tag{2.7}$$

Where p is the pixel location in the foreground.

Erosion of a point retains the minimum of all points in its neighborhood and the neighborhood is defined by the structuring element. Erosion of an image I by a structuring element H is defined as

$$I \ominus H = \{p | H_p \subseteq I\} \tag{2.8}$$

Where p is the pixel location in the foreground. Erosion can also be computed as the dilation of the background.

2.2.5 Boundary Extraction

Boundary Extraction has been performed to determine the boundary of the regurgitant jet obtained as the result of performing morphological operations. The boundary of an segmented image *I* can be extracted by first eroding the image *I* with a structuring element B and then performing the set difference between the image *I* and its erosion. This can be expressed as below,

$$\beta(A) = A - (A \ominus B) \tag{2.9}$$

Where β (A) denotes the boundary of the image I.

2.2.6 Area Calculation

In the end, the area of the segmented image is calculated by counting the pixels under the boundary.

2.3 MR Severity Evaluation

MR Severity Evaluation is performed on the basis of the standards for the regurgitant jet of MR prescribed by the American Heart Association. The number of pixels present in the segmented mosaic pattern is calculated and based on the parameters like screen resolution and dots per inch of the display the area of the regurgitant jet is calculated.

2.3.1. Pixel Counting

Pixel counting has been performed on the binary image, obtained as the result of Morphological operations. At the end of performing morphological operations, the resultant image is binary in nature and the pixels present inside the regurgitant jet area have the intensity level 255. The number of pixels is calculated to determine the area of the mosaic pattern and hence to classify the severity of MR according to the estimated area.

$$N_p = \begin{cases} N_p + 1, if\ p(x,y) = 255 \\ N_p, if\ p(x,y) < T \end{cases} \quad (2.10)$$

Where *Np* denotes the number of pixels, *p(x, y)* denotes the pixel value. Whenever the value of the pixels in the image equals to the white intensity level then the number of pixels is incremented by 1.

2.3.2. Severity Determination

The regurgitant jet area is calculated based on the Number of pixels *Np*, resolution of the screen on which the image is displayed and the dots per inch value of the display device. Upon calculation of the area of the mosaic pattern, the severity of MR has been classified based on the standards prescribed by American Heart Association/ American College of Cardiology (AHA/ACC). According to the guidelines of AHA/ACC, the severity of MR of a patient is evaluated as mild if the jet area is < 4 cm^2, as moderate when the jet area is > 4 cm^2 and < 8 cm^2 and as severe when the jet area is > 8 cm^2.

CHAPTER 3

RESULTS AND DISCUSSIONS

The MR in the echocardiographic images can be seen in three perspectives: apical two chambers (A2C), apical four chambers (A4C) and parasternal long axis (PLAX). The A2C view delineates the anterior and inferior walls of the left ventricle. The A4C view demonstrates all the four chambers of the heart. The A4C view is thought to be the best view by the clinicians to study in how and to visualize the apex of the left ventricle. The PLAX view helps in the measurement of the size of both left and right ventricle and also for the interpretation of the VHD. In the present days, all the three perspectives of the patients are utilized by the clinicians for diagnosing the severity of MR [47].

A total of 75 color Doppler ultrasound images of heart patients suffering from MR have been used in this study. These images were collected from the department of cardiology, Swami Rama Himalayan University (SHRU), Dehradun, India. The ultrasound images used for the evaluation of MR were recorded by Philips ultrasound machine equipped with multi-frequency transducers of 2-5 MHz range. These ultrasound images were collected in all the three views namely A2C, A4C and PLAX view. The size of the images utilized for severity examination of MR is 800 × 600 pixels. The grading of the MR images in three classes, i.e. mild, moderate and severe have been done by the experienced cardiologists. The proposed method for the evaluation of the severity of MR is applied on the color Doppler images of about 25 patients in all the three views namely mild, moderate and severe having different levels of severity and results are discussed below.

3.1 RESULTS OBTAINED FOR A2C VIEW TYPE IMAGES

The proposed method for the evaluation of severity of MR is applied on the color Doppler images of patients in all the three views having different levels of severity and results are discussed below. RGB color space of the input image in A2C view is shown in the fig.3.1. HSV color space of the input image in A2C view is shown in the fig.3.2. YCbCr color space of the input image in A2C view is shown in the fig.3.3.

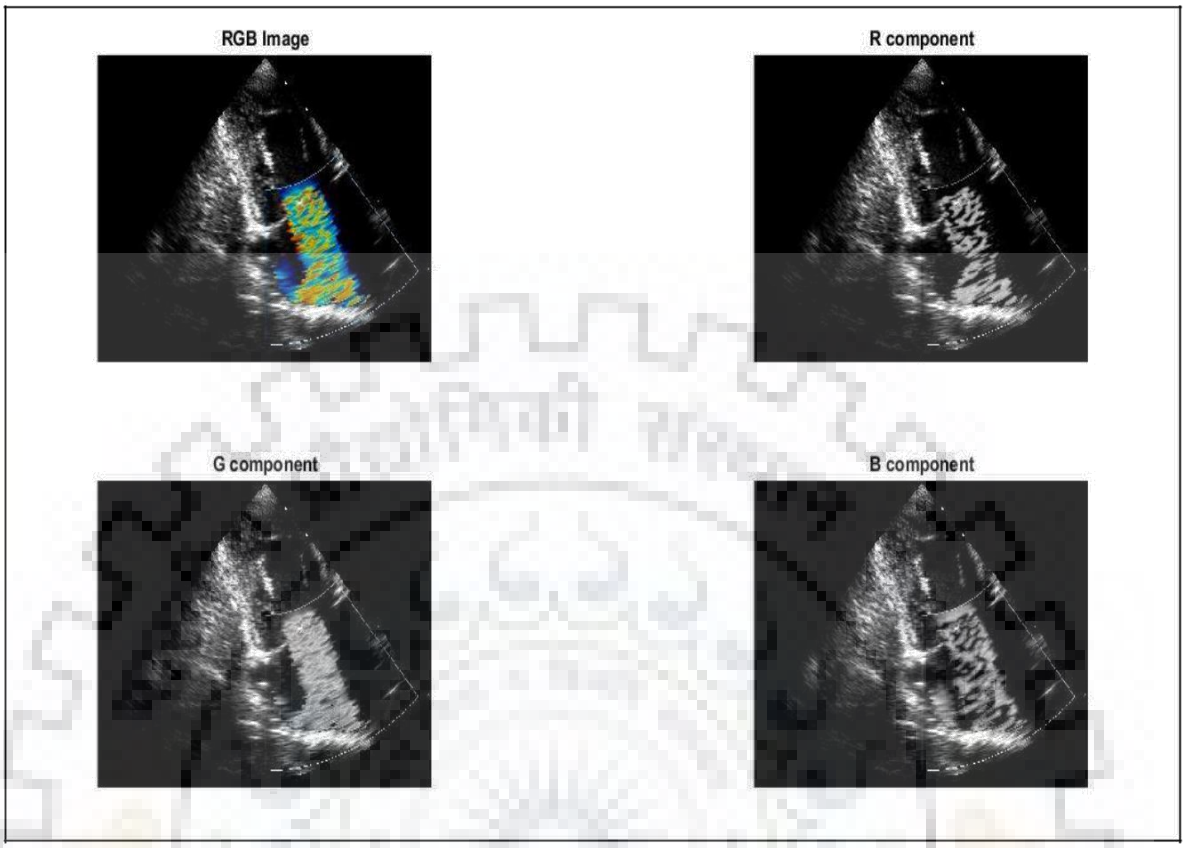

Figure 3.1 RGB color space of the input image in A2C view.

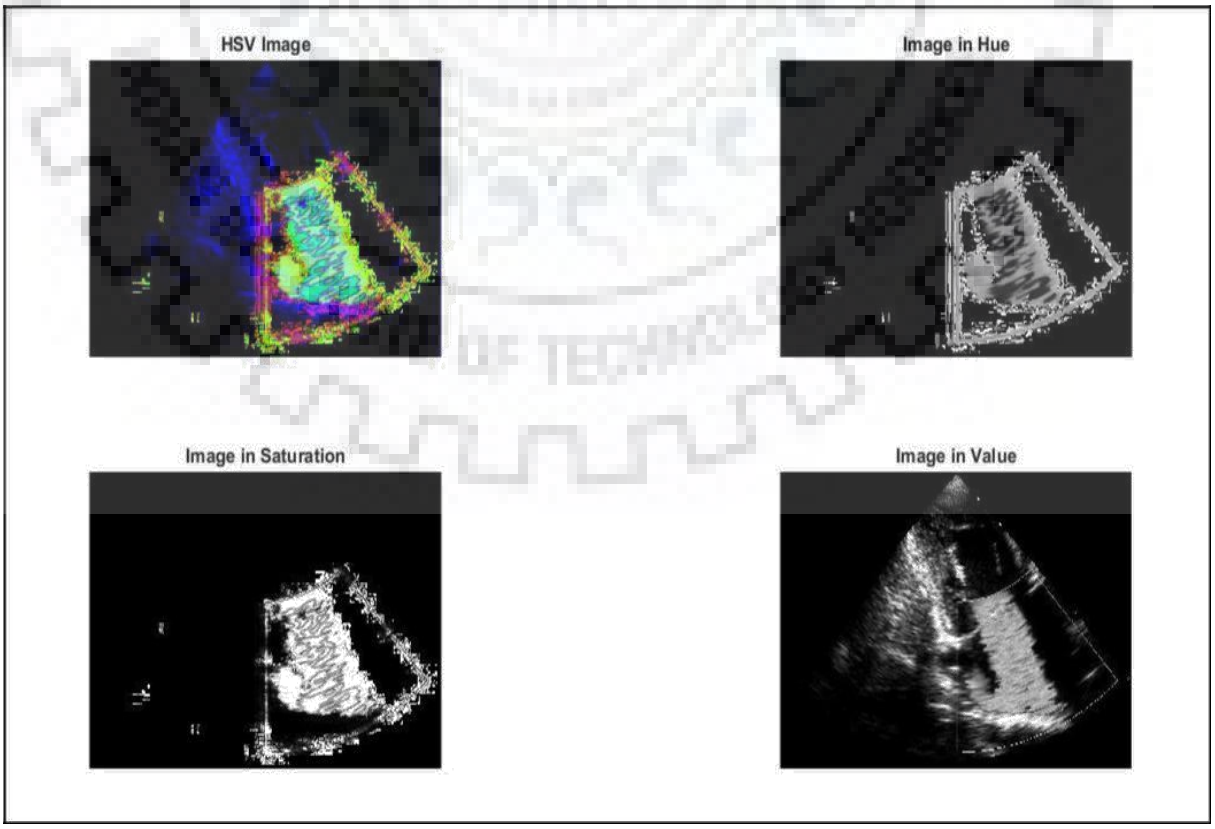

Figure 3.2 HSV color space of the input image in A2C view.

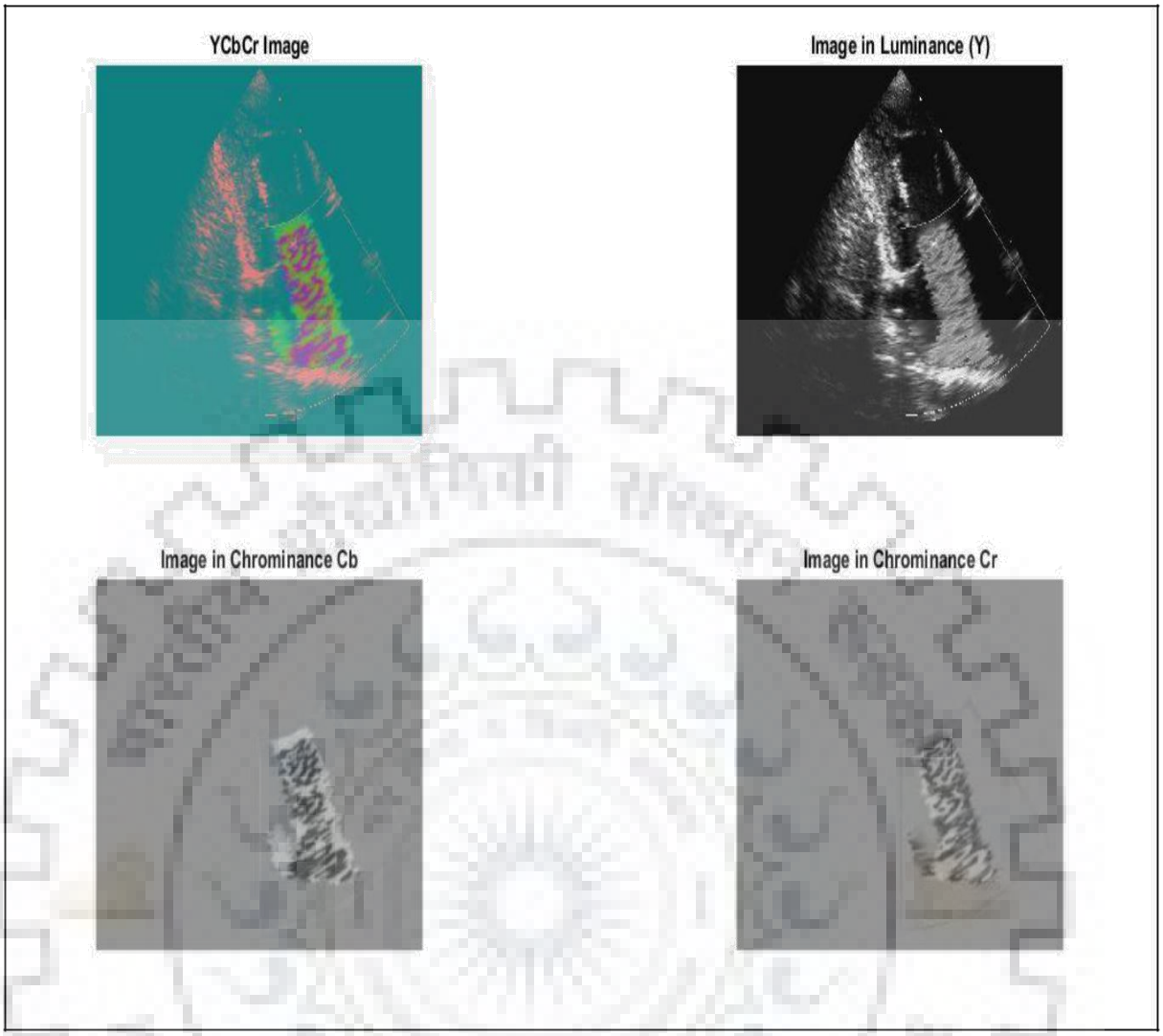

Figure 3.3 YCbCr color space of the input image in A2C view.

YIQ and Gray scale color spaces of the input image in A2C view is shown in the fig.3.4.

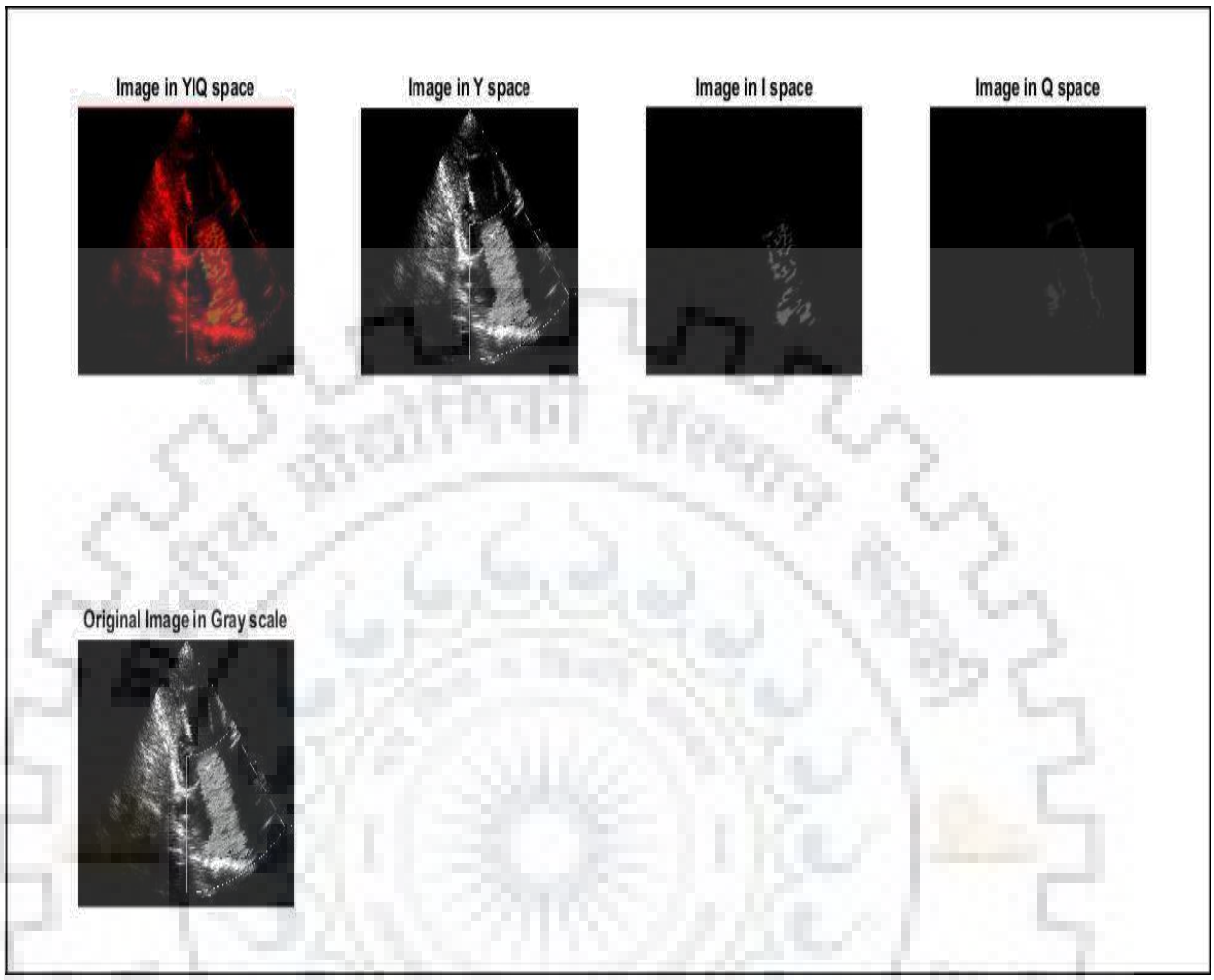

Figure 3.4 YIQ and Gray scale color spaces of the input image in A2C view

Output of the proposed algorithm after each step in A2C view is shown in the fig.3.5.

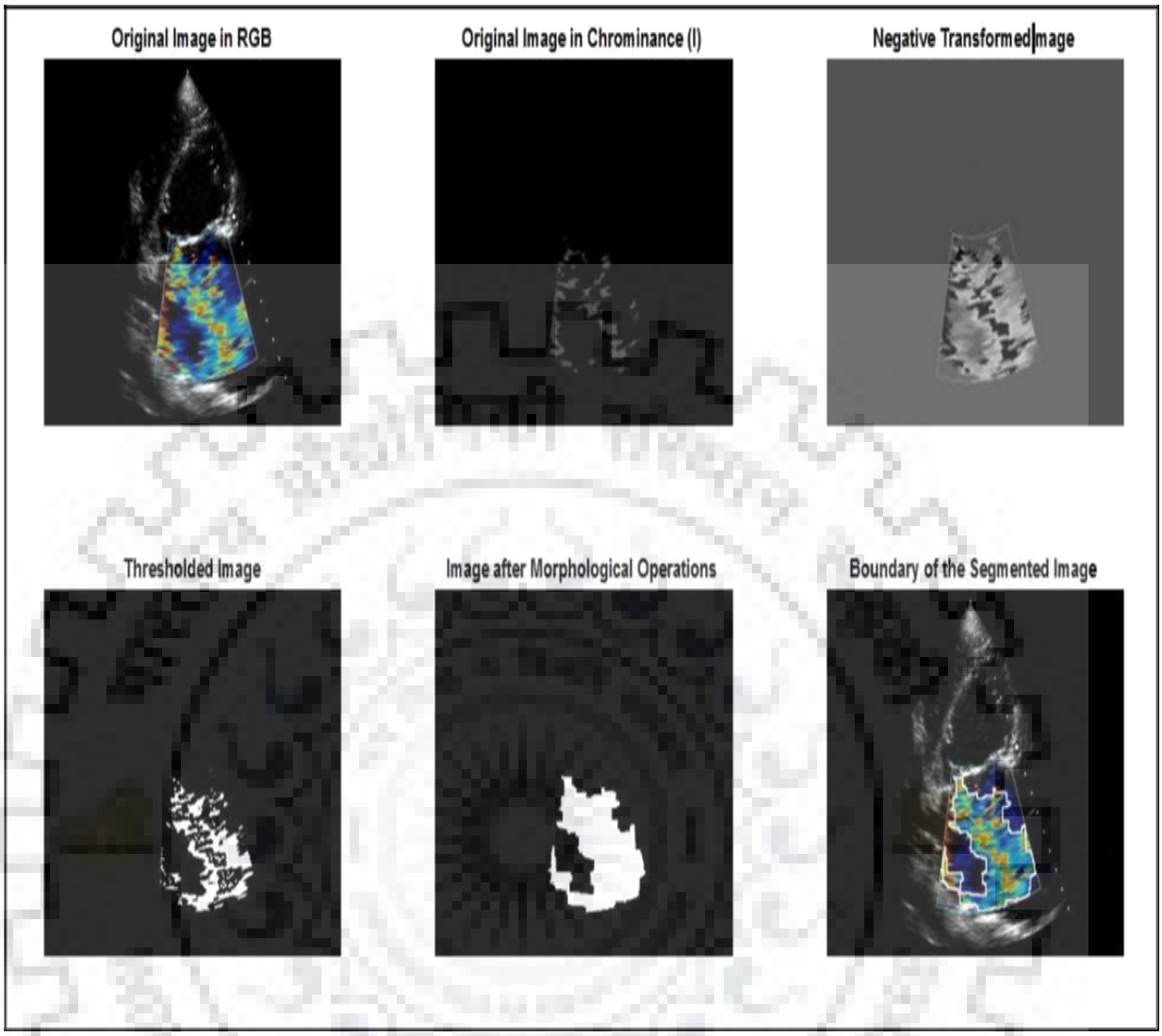

Figure 3.5 Output of the proposed algorithm after each step in A2C view

The results obtained for patients in A2C view having different levels of severity are shown in the fig.3.6.

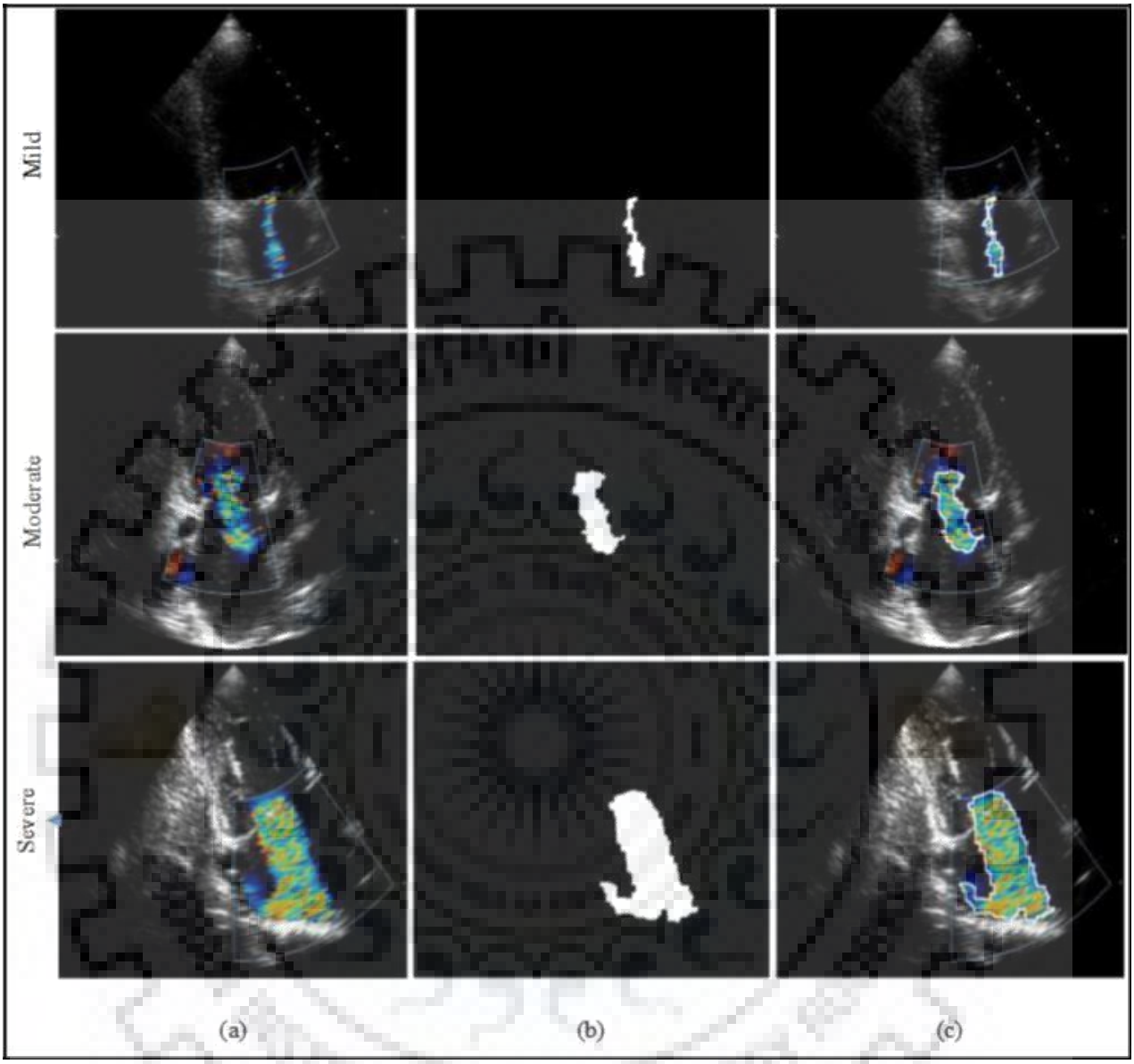

Figure 3.6 MR Severity in A2C view. (a) Original Image in RGB. (b) MR Segmented Image (c) Regurgitation jet area boundary detection results.

In the above figure, an example is shown for each case of severity of MR namely Mild, Moderate and Severe. The original image is the one obtained from the ultrasound scanner. The segmented image is obtained on application of the proposed segmentation algorithm to the original image and finally, the boundary of the segmented image is superimposed on the original images and is shown as the boundary. In the similar manner the results obtained for patients in A4C view and PLAX view having different levels of severity are shown in the subsequent figures.

3.2 RESULTS OBTAINED FOR A4C VIEW TYPE IMAGES

RGB color space of the input image in A4C view is shown in the fig.3.7. HSV color space of the input image in A4C view is shown in the fig.3.8. YCbCr color space of the input image in A4C view is shown in the fig.3.9.

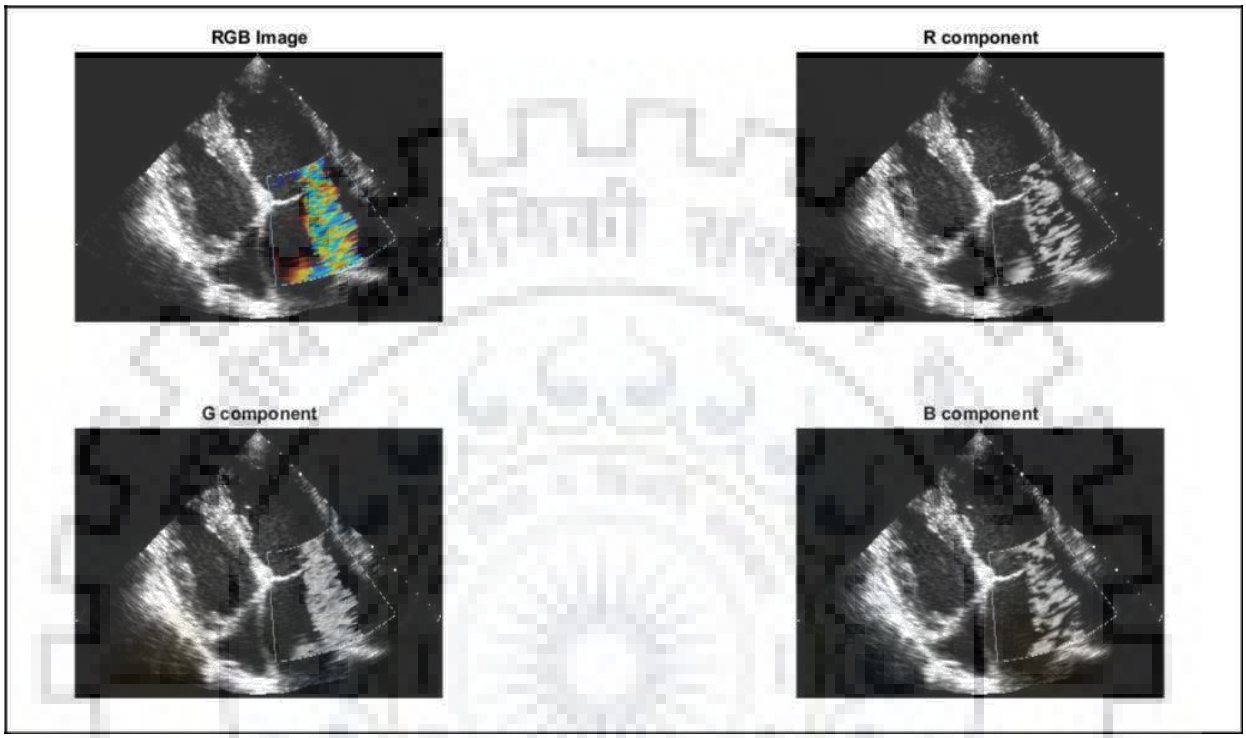

Figure 3.7 RGB color space of the input image in A4C view

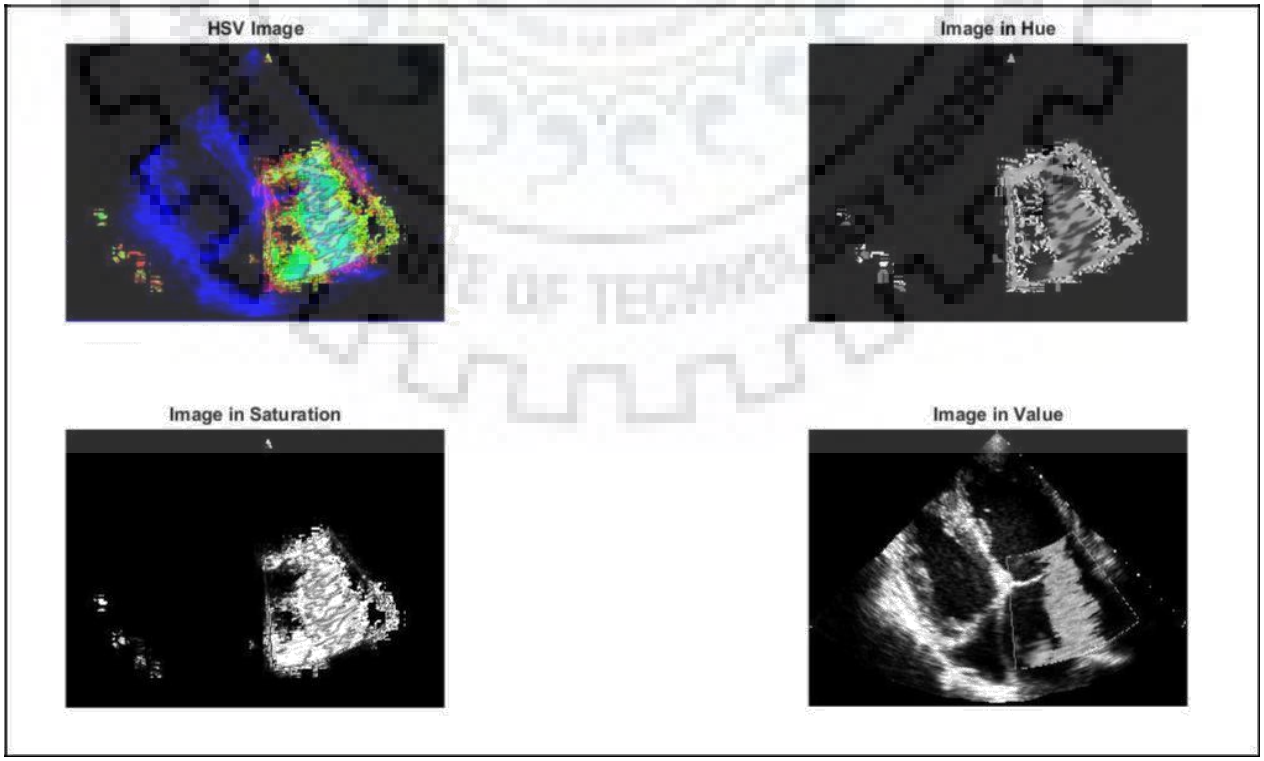

Figure 3.8 HSV color space of the input image in A4C view

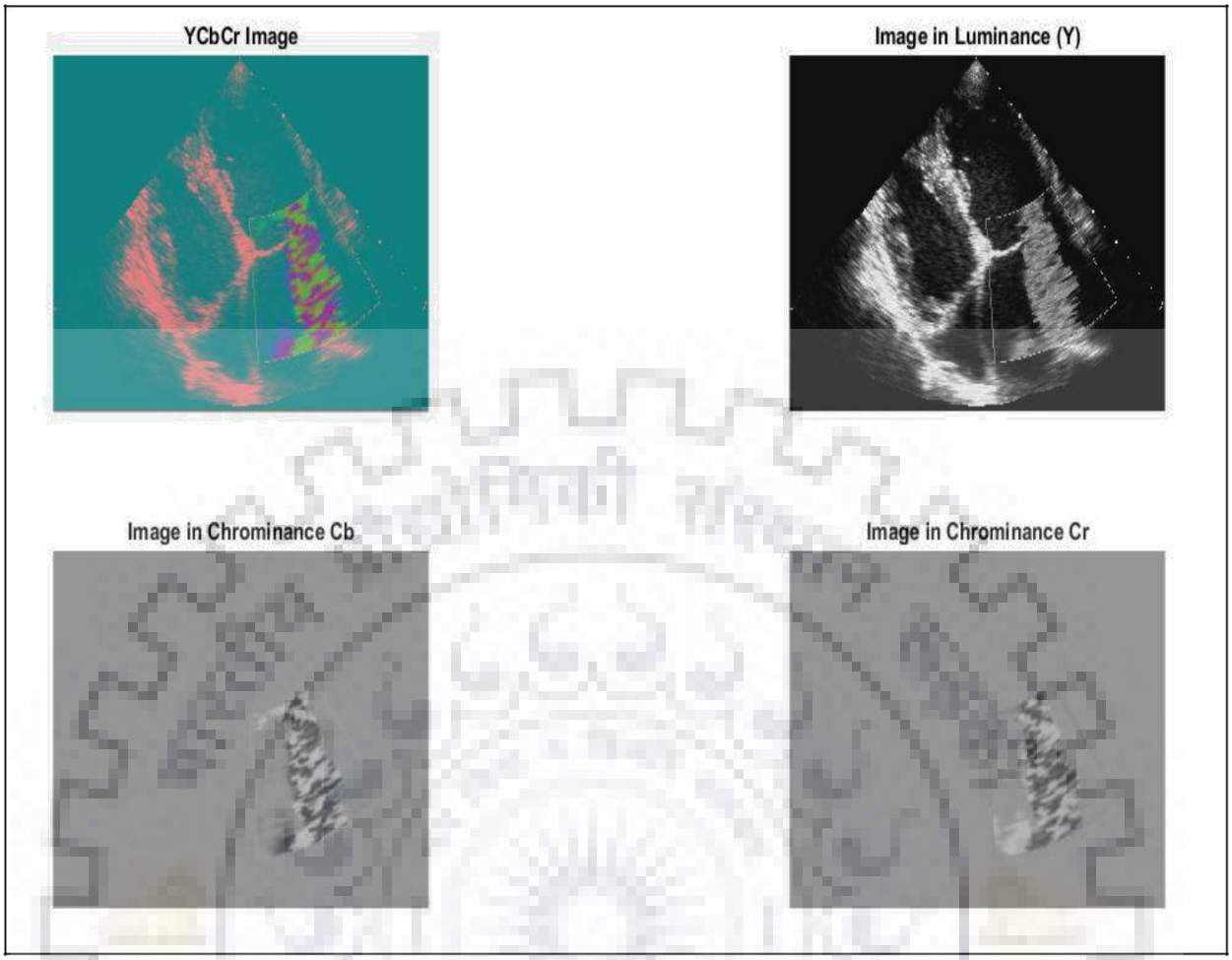

Figure 3.9 YCbCr color space of the input image A4C view

YIQ and Gray scale color spaces of the input image in A4C view is shown in the fig.3.10.

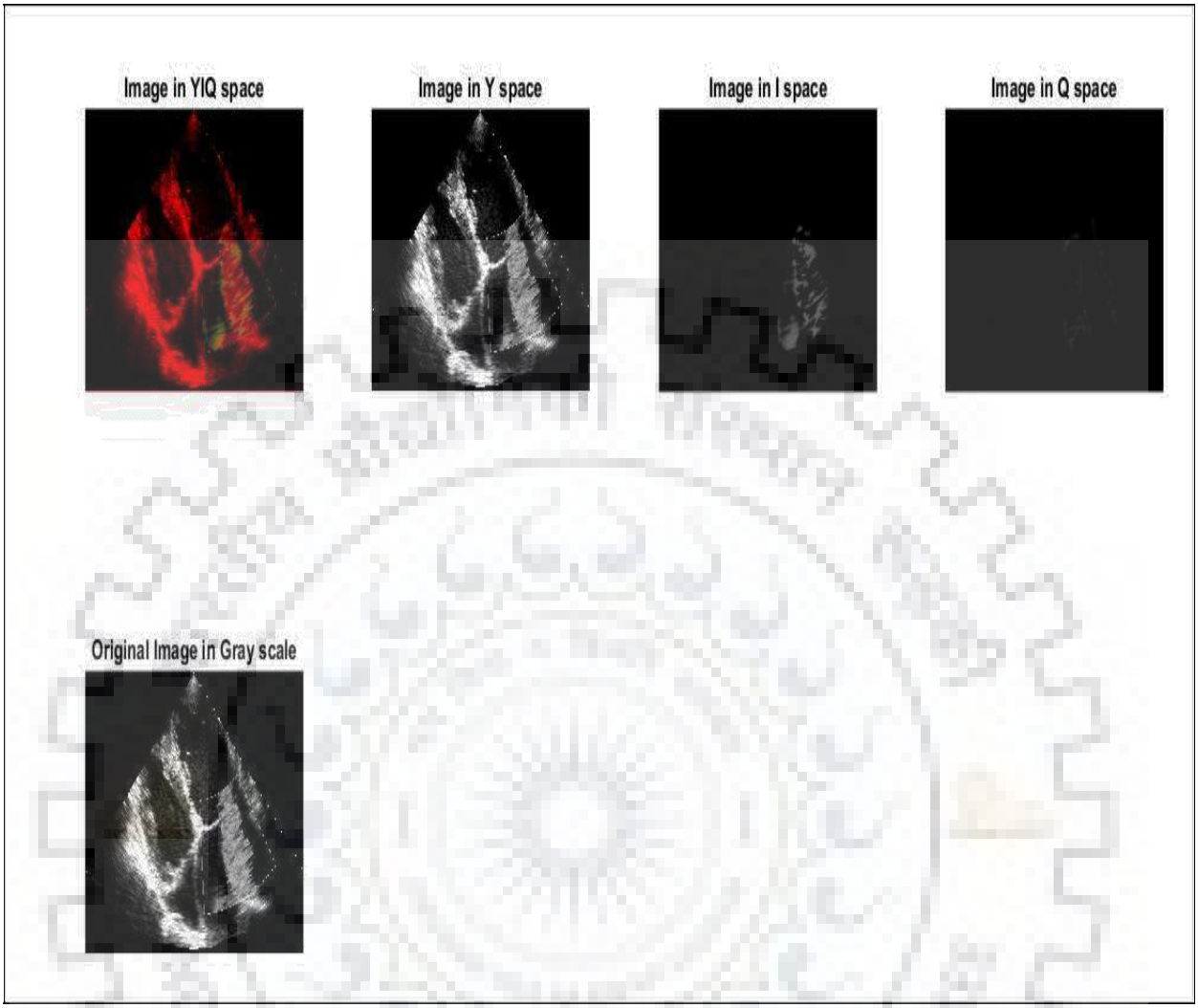

Figure 3.10 YIQ and Gray scale color space of the input image A4C view

Output of the proposed algorithm after each step in A4C view is shown in the fig.3.11.

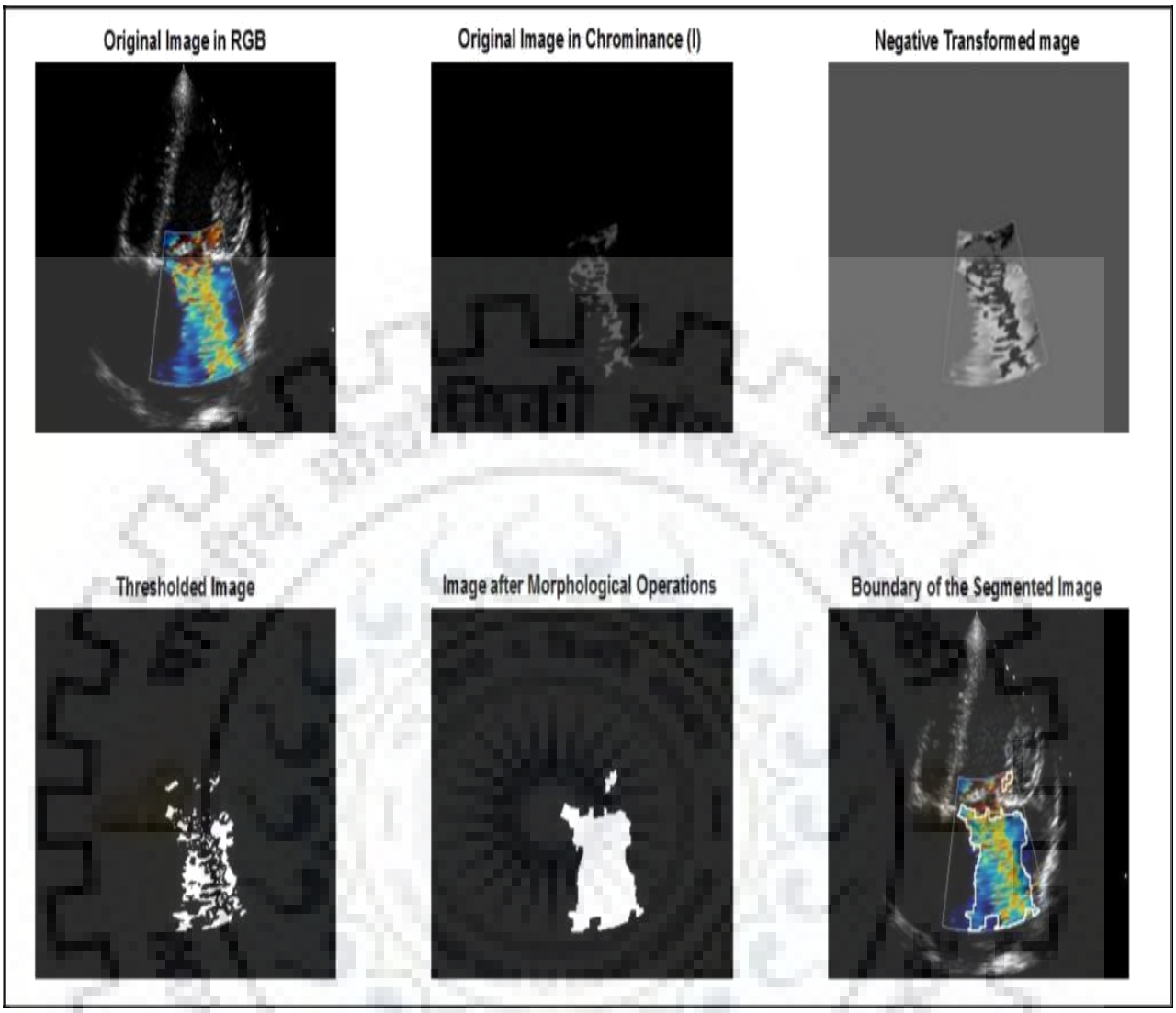

Figure 3.11 Output of the proposed algorithm after each step in A4C view

The results obtained for patients in A4C view, having different levels of severity are shown in the fig.3.12

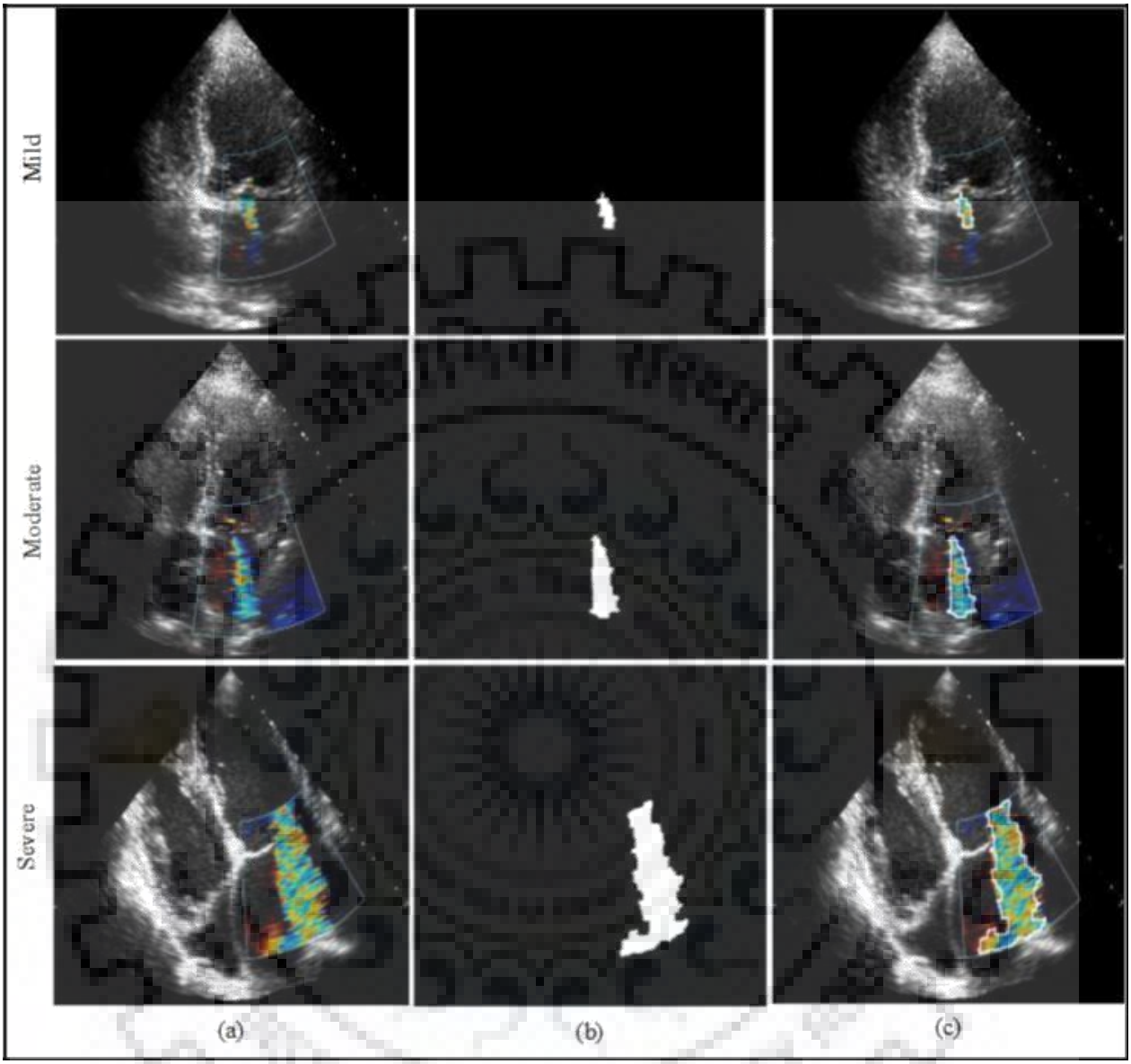

Figure 3.12 MR Severity in A4C view. (a) Original Image in RGB. (b) MR Segmented Image (c) Regurgitation jet area boundary detection results.

3.3 RESULTS OBTAINED FOR PLAX VIEW TYPE IMAGES

RGB color space of the input image in PLAX view is shown in the fig.3.13. HSV color space of the input image in PLAX view is shown in the fig.3.14. YCbCr color space of the input image in PLAX view is shown in the fig.3.15.

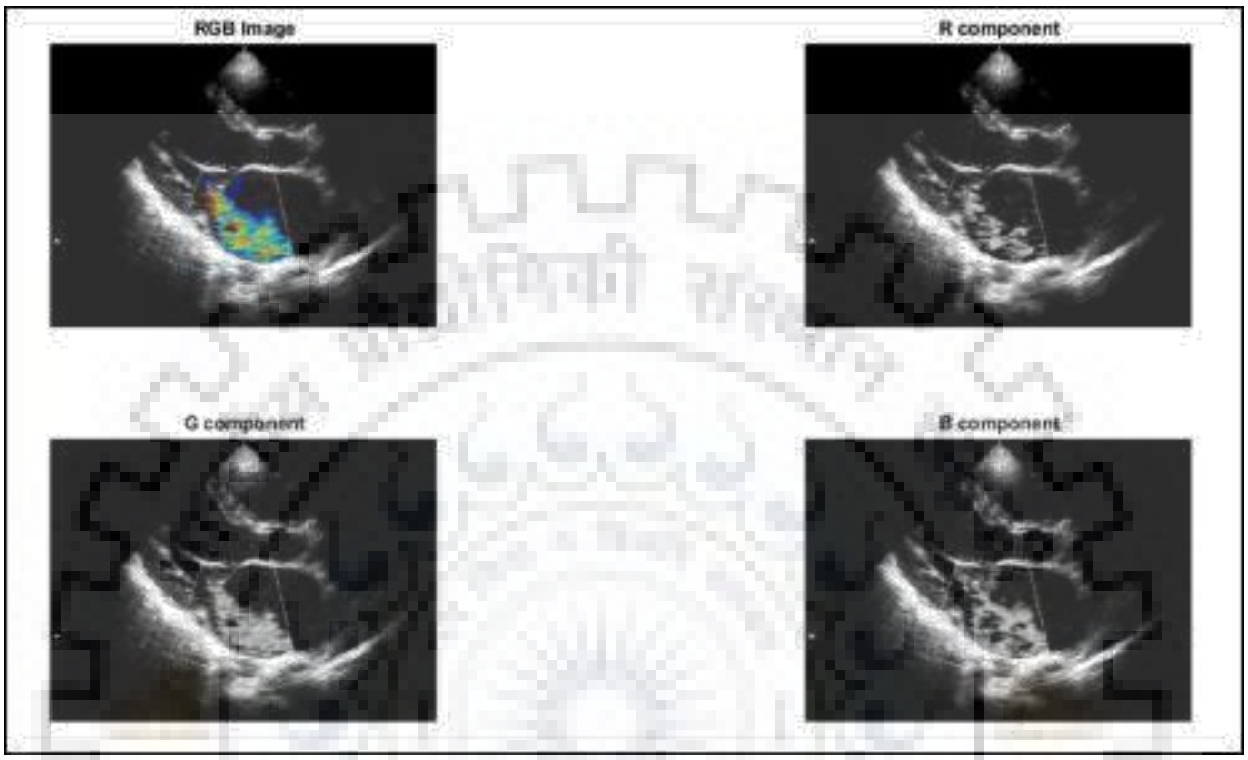

Figure 3.13 RGB color space of the input image in PLAX view

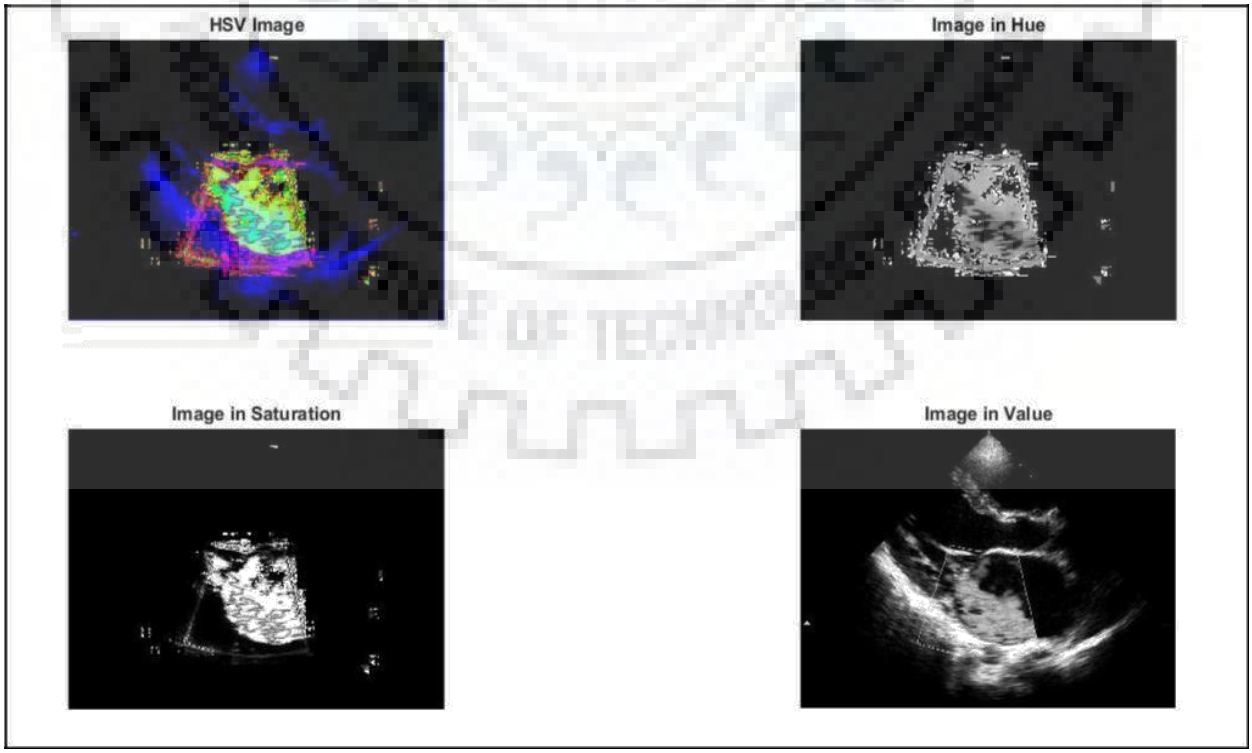

Figure 3.14 HSV color space of the input image in PLAX view

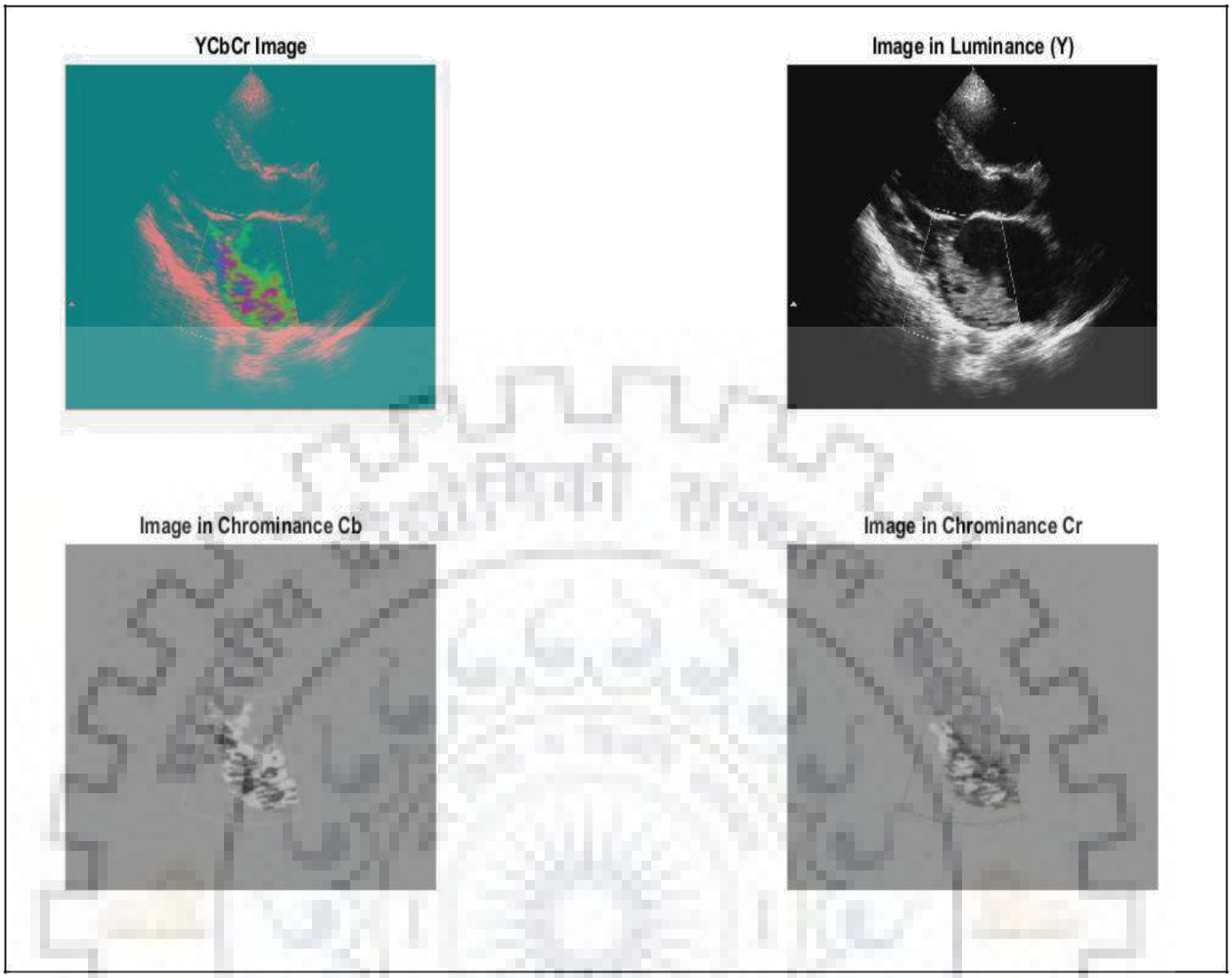

Figure 3.15 YCbCr color space of the input image in PLAX view

YIQ and Gray scale color spaces of the input image in PLAX view is shown in the fig.3.16.

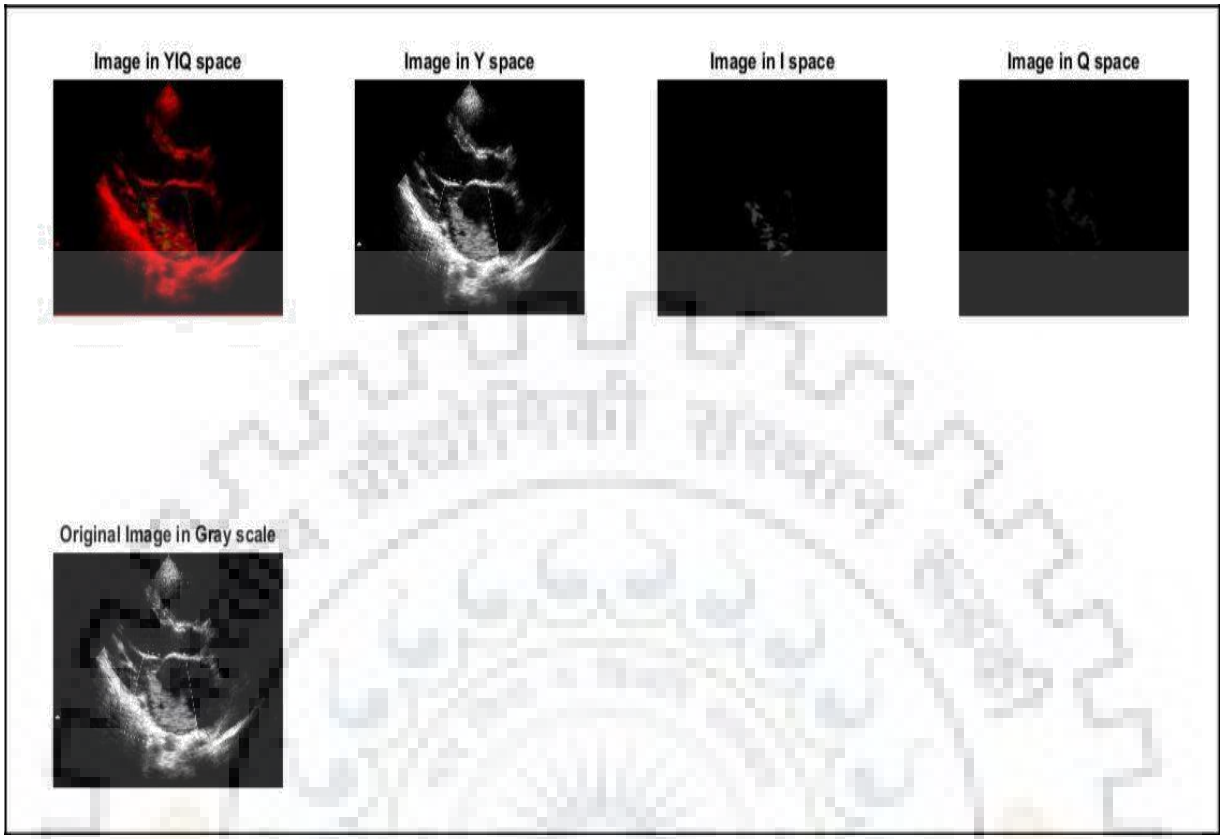

Figure 3.16 YIQ color space and Gray scale of the input image in PLAX view

Output of the proposed algorithm after each step in PLAX view is shown in the fig.3.17.

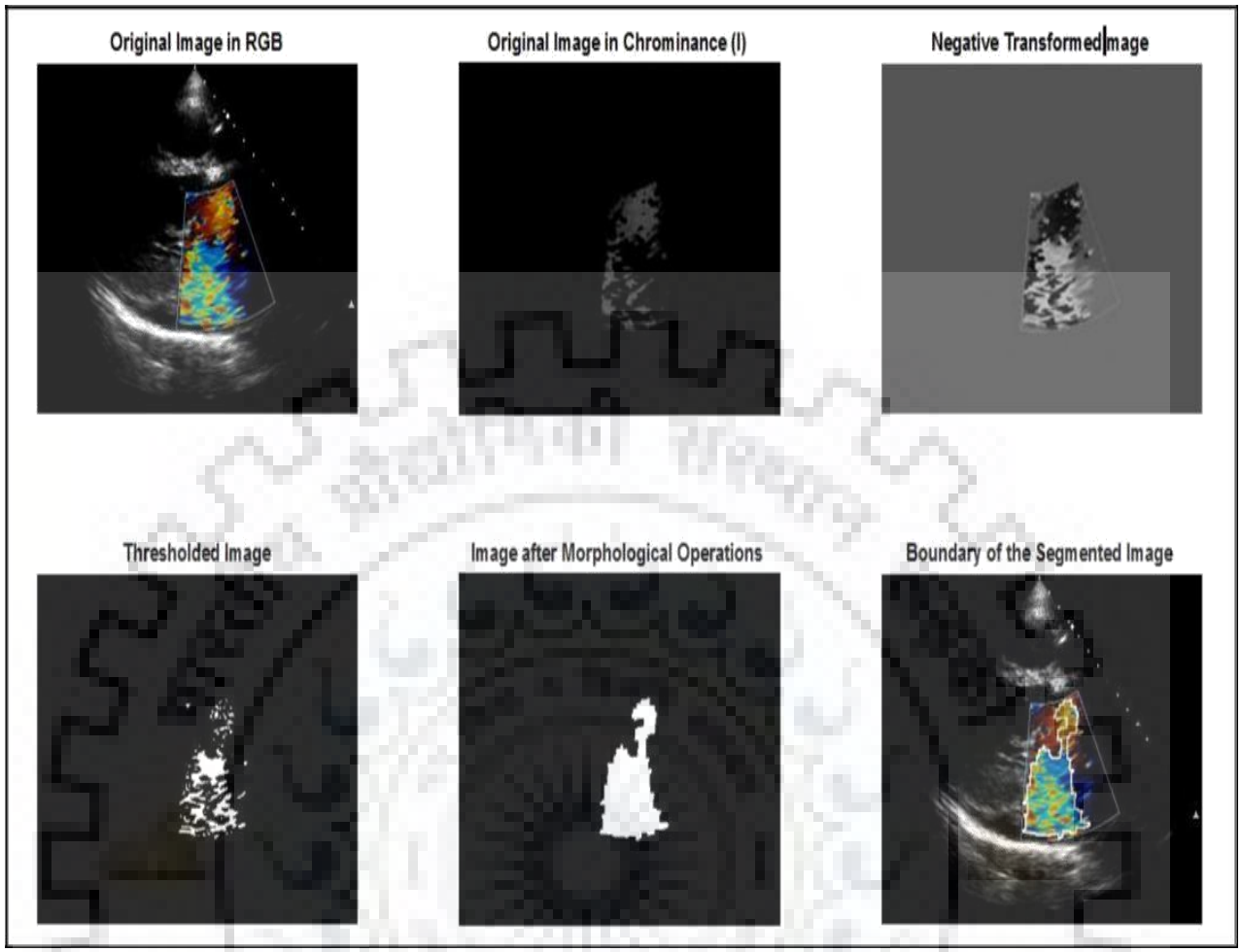

Figure 3.17 Output of the proposed algorithm after each step in PLAX view

The results obtained for patients in PLAX view, having different levels of severity are shown in the fig.3.18

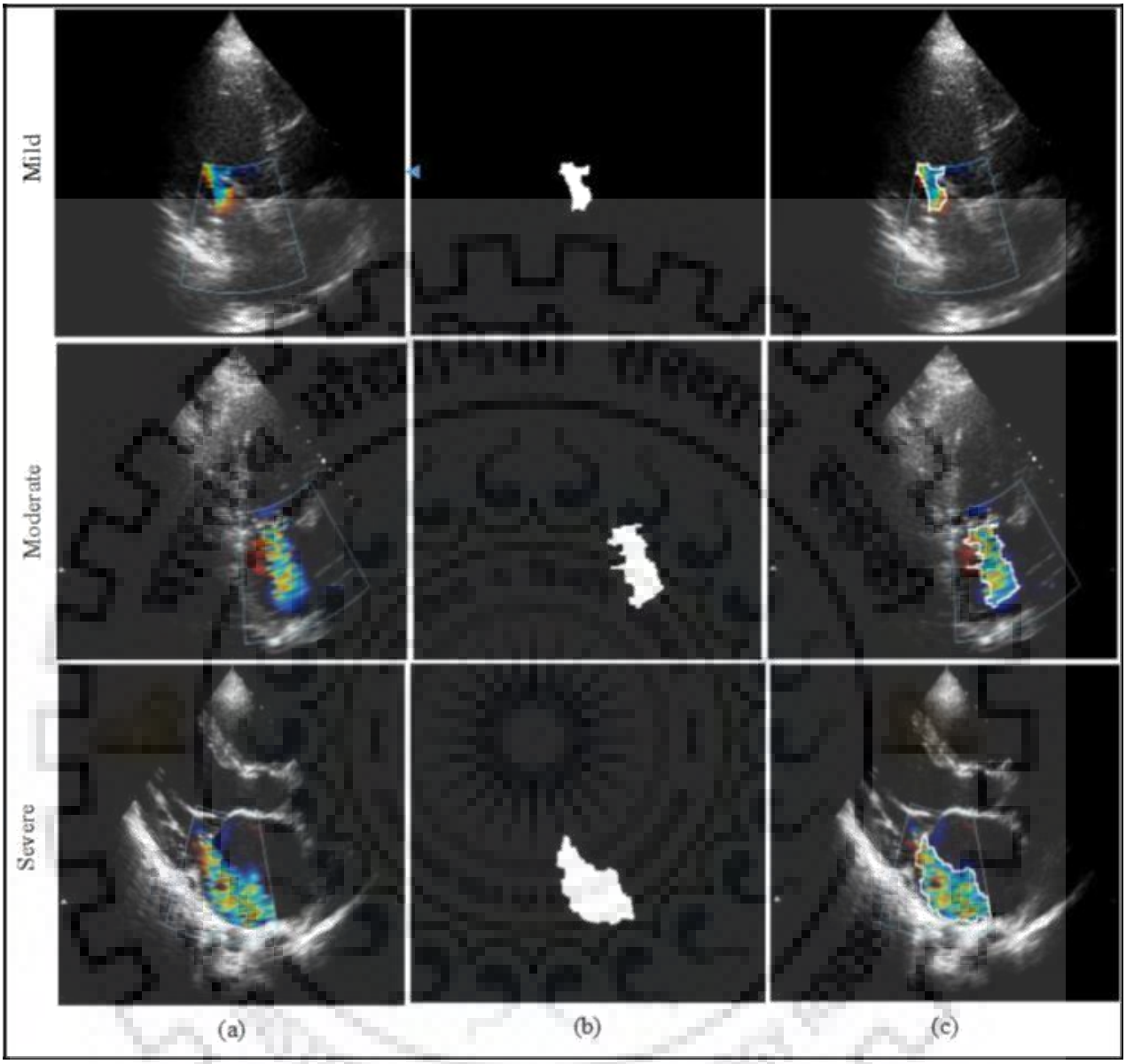

Figure 3.18 MR Severity in PLAX view. (a) Original image in RGB. (b) MR Segmented image (c) Regurgitation jet area boundary detection results.

Based on the proposed method the number of pixels present in the segmented mosaic pattern is determined and based on the resolution of the screen and dots per inch of the display the area of the regurgitant jet is determined in cm2. The severity evaluation has been performed based on the standards prescribed by AHA/ACC. The results obtained for the proposed method has been cross verified with the severity level obtained by the manual method based on the assessment of the cardiac. And the results are found to be satisfactory.

The calculated value of the regurgitant jet area in case of 25 patients is shown in fig.3.19, in the form of graphical representation.

Number of Patients Vs Regurgitant Jet Area

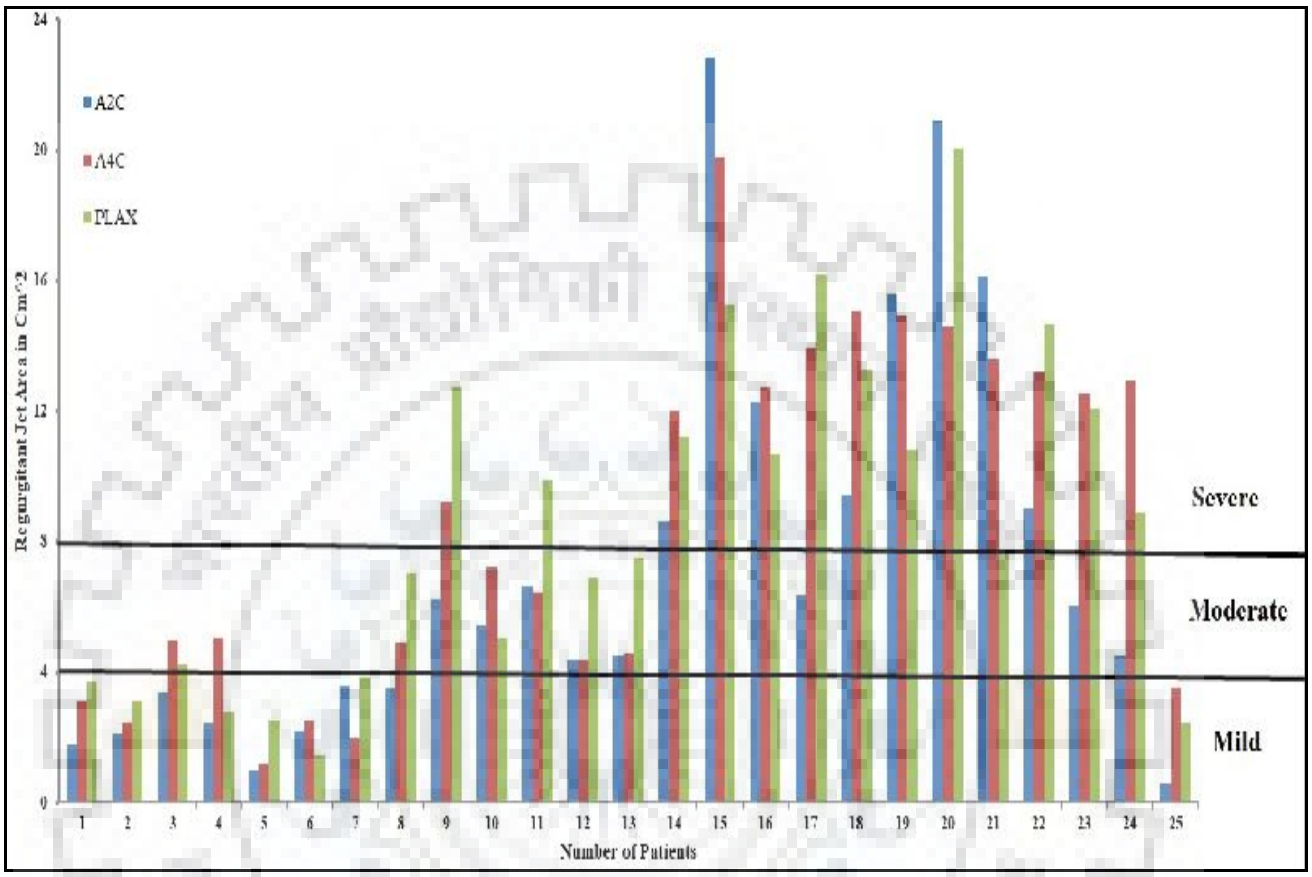

Figure 3.19 Severity classification based on calculated area

The x-axis in the graph denotes the number of patients and the y-axis denotes the regurgitant jet area in cm^2. Reference lines are marked at 4 cm^2 and 8 cm^2 to distinguish the severity level of the patients namely mild, moderate and severe. When the regurgitant jet area is less than 4 cm^2 the case is classified as mild and when the jet area falls within a range of 4 cm^2 to 8 cm^2 the case is classified as moderate and for the jet area values greater than 8 cm^2 the case is classified as severe. The classification has been done on the basis of the standards prescribed by the American Heart Association/ American College of Cardiology (AHA/ACC). When the calculated values of the regurgitant jet area were compared with the values obtained from the manual method the results were found to be in a close match. The regurgitant jet area calculated from the proposed algorithm is correlated with the classification of MR severity and the results are tabulated below.

Table 1: Results of the proposed algorithm

Patients	Severity (Manual Method)			No of Pixels			Regurgitant Jet Area (cm^2)		
	A2C	A4C	PLAX	A2C	A4C	PLAX	A2C	A4C	PLAX
1	Mild	Mild	Mild	1563	2723	3239	1.793	3.123	3.715
2	Mild	Mild	Mild	1875	2133	2696	2.151	2.447	3.092
3	Mild	Moderate	Moderate	2946	4308	3663	3.379	4.941	4.201
4	Mild	Moderate	Mild	2119	4413	2394	2.43	5.0617	2.746
5	Mild	Mild	Mild	870	1005	2213	0.998	1.153	2.538
6	Mild	Mild	Mild	1928	2166	1277	2.211	2.484	1.465
7	Mild	Mild	Mild	3136	1696	3367	3.597	1.945	3.862
8	Mild	Moderate	Moderate	3052	4250	6127	3.501	4.875	7.028
9	Moderate	Severe	Severe	5453	8053	11126	6.255	9.237	12.762
10	Moderate	Moderate	Moderate	4712	6278	4414	5.405	7.201	5.063
11	Moderate	Severe	Severe	5767	5613	8602	6.615	6.438	9.866
12	Moderate	Moderate	Moderate	3792	3780	6037	4.349	4.336	6.924
13	Moderate	Moderate	Moderate	3912	4004	6565	4.487	4.593	7.53
14	Severe	Severe	Severe	7524	10448	9786	8.63	11.984	11.225
15	Severe	Severe	Severe	19942	17277	13301	22.873	19.817	15.256
16	Severe	Severe	Severe	10740	11142	9337	12.319	12.78	10.709
17	Moderate	Severe	Severe	5532	12148	14129	6.345	13.934	16.206
18	Severe	Severe	Severe	8252	13170	11579	9.465	15.106	13.281
19	Severe	Severe	Severe	13608	13005	9469	15.608	14.917	10.861
20	Severe	Severe	Severe	18217	12708	17471	20.895	14.576	20.039
21	Severe	Severe	Moderate	14092	11860	6613	16.164	13.603	7.585
22	Severe	Severe	Severe	7834	11508	12771	8.986	13.199	14.648
23	Moderate	Severe	Severe	5260	10941	10547	6.033	12.549	12.097
24	Moderate	Severe	Severe	3957	11246	7755	4.5387	12.8992	8.895
25	Mild	Mild	Mild	494	3067	2116	0.5666	3.5178	2.4271

Results of the proposed algorithm in comparison with manual method are depicted above in table.1.

CHAPTER 4

CONCLUSION

4.1 CONCLUSION

The proposed method for segmentation of the mosaic pattern of MR in color Doppler ultrasound images was discussed in detail. The proposed method helps in evaluating the severity of MR based on the area of the mosaic pattern obtained from the segmented image. The results were compared with the manual method, used by clinicians in the present days and was found that there was no misevaluation in the severity of MR. The proposed method based on the color space model overcomes the need of despecking techniques which is used as a pre-processing step in most of the algorithms used for segmentation of ultrasound images. Thus, the proposed algorithm reduces the computation time, memory and also eliminates the need for manual intervention which is prevalent in the method used in the existing days. The results of the proposed method suggest that the accuracy of evaluation of severity level of MR in all the three view of the patient can be done with high accuracy.

REFERENCES

[1] Kamaljeet Kaur, "Digital Image Processing in Ultrasound Images", *International Journal on Recent and Innovation Trends in Computing and Communication*, Vol 1,No.4 , pp 388-393, March 2013.

[2] Krzysztof Iniewski, "MEDICAL IMAGING Principles, Detectors, and Electronics", New Jersey: John Wiley & Sons, 2009, pp 167-190.

[3] Arash Anvari, Flemming Forsberg and Anthony E. Samir, "A Primer on the Physical Principles of Tissue Harmonic Imaging", *RadioGraphics*, Vol 35, No.7, pp 1955-1964, November 2015.

[4] James F. Havlice and Jon C. Taenzer, "Medical Ultrasonic Imaging: An Overview of Principles and Instrumentation", *Proceedings of the IEEE*, Vol 67, No. 4,pp 620-641, May 1979.

[5] Carovac A, Smajlovic F and Junuzovic D, "Application of Ultrasound in Medicine", *Acta Inform Med*, Vol 19, No.3, pp 168-171, September 2011.

[6] Robert W. Coatney, "Ultrasound Imaging: Principles and Applications in Rodent Research", *ILAR J*, Vol.42, No.3, pp 233-247, March 2001.

[7] Darshana De, "Emerging Trends in Ultrasound Imaging", Toshiba Medical Systems, Otawara, Japan, October 25, 2012.

[8] Pooja Rani and Rakesh Verma, "A Review on Ultrasound Image Segmentation Techniques", *International Journal of Advanced Research in Electronics and Communication Engineering* , Vol.4, No.8, pp 2248-2251, August 2015.

[9] J. S. Lee, "Speckle analysis and smoothing of synthetic aperture radar images," *Comput.Graph.Image Process*, Vol.17,No.1, pp. 2432, Sep.1981.

[10] D. T. Kuan, A. A. Sawchuk, T. C. Strand, and P. Chavel, "Adaptive noise smoothing filter for images with signal-dependent noise," *IEEE Trans. Pattern Anal. Mach. Intell.*, Vol. 7, No. 2, pp. 16577, Mar. 1985.

[11] Juerg Tschirren, Ronald M. Lauer, and Milan Sonka,"Automated Analysis of Doppler Ultrasound Velocity Flow Diagrams," *IEEE Transactions on Medical Imaging*, Vol. 20, No. 12, Dec. 2001.

[12] Z. Dengwen, and C. Wengang, "Image denoising with an optimal threshold and neighbouring window," *Pattern Recognit. Lett.*, Vol. 29, no. 11, pp. 169-497, Aug. 2008.

[13] J. L. Mateo, and A. Fernandez-Caballero, "Finding out general tendencies in speckle noise reduction in ultrasound images," *Expert Syst. Appl.*,Vol. 36, pp. 697-778, May 2009.

[14] J. Zhang, C. Wang, and Y. Cheng, "Comparison of despeckle filters for breast ultrasound images," *Circuits Syst. Signal Process*.,pp. 124, June 2014.

[15] Ashish Thakur and R.S. Anand, "Image quality based comparative evaluation of wavelet filters in ultrasound speckle reduction," *Digital Signal Processing*, Vol. 15, pp.455–465, Feb 2005.

[16] Sanyam Anand, Amitabh Sharma and Akshay Girdhar, "Non decimated Wavelet Based new Threshold Technique for Eliminating Speckle Noise in Ultrasound Images," *International Conference on Computational Techniques and Artificial Intelligence*, pp.101-108, Oct 2011.

[17] J. A Noble and D Boukerroui, " Ultrasound Image Segmentation: A Survey" *IEEE Transactions on Medical Imaging*, Vol. 25, No. 8, pp.987-1010, August 2006.

[18] J G. Thomas, R A Peters II and P Jeanty, " Automatic Segmentation of Ultrasound Images using Morphological Operators" *IEEE Transactions on Medical Imaging*, Vol. 10, No. 2, pp. 180-186, June 1991.

[19] J Cheng, S W Foo and S M. Krishnan, " Watershed-Presegmented Snake for boundary detection and tracking of left ventricle in Echocardiographic images" *IEEE Transactions on Information Technology in Biomedicine,* Vol. 10, No. 2, pp. 414-416, April 2006.

[20] E R. Wolfe, E J. Delp, C R. Meyer, F L. Bookstein and A J. Buda, "Accuracy of Automatically Determined borders in Digital Two- Dimensional Echocardiography using a cardiac phantom" *IEEE Trans. Medical Imaging*, Vol. 6, No. 4,pp. 292-297, Dec. 1987.

[21] C Lamberti , A Martelli and A Guidazzoli, " Postprocessing techniques for 2D Echocardiographic Imaging" *IEEE Engineering In Medicine & Biology Society 10th Annual International Conference*, pp. 450-452, 1988.

[22] C Sheng, Y Xin, Y Liping & S Kun, " Segmentation in echocardiographic sequences using shape-based snake model combined with generalized Hough transformation" *The International Journal of Cardiovascular Imaging*, Vol.22, pp.33–46, 2006.

[23] I Miki, S Krucinski, and J D. Thomas, "Segmentation and Tracking in Echocardiographic Sequences: Active Contours Guided by Optical Flow Estimates' *IEEE Transactions on Medical Imaging,* Vol. 17, No. 2, April 1998.

[24] E Boonchieng, W Boonchieng and R Kanjanavanit, " Edge detection and segmentation for two dimensional Echocardiograms' *IEEE Journal of Computers in Cardiology,* Vol. 31, pp. 541-544, 2004.

[25] E A R Humadal and S.A.R. Abu-Bakar, "Automatic Coronary Artery Detection In Echocardiogram Image' *IEEE International Conference on Signal Processing and Communications*, pp. 24-27, Nov. 2007.

[26] Xi Wang, Ronny Hansch, Lizhuang Ma and Olaf Hellwich, "Comparison of different colour spaces for Image Segmentation using Graph-cut" *International conference on Computer vision Theory an Applications*, pp. 301-308, 2014.

[27] Kalpana Saini, M.L. Dewal and Manojkumar Rohit, " Detection of Mitral Regurgitation Severity using Color Histogram" *International Journal of Research in Biological Sciences,* Vol. 3, No. 2, pp. 102-108, May 2013.

[28] K.R. Ananth and P. Navaneethan, "Modified Multiresolution Medical Image Segmentation based on Wavelet Transform" *International Journal of Computer Science and Mobile Computing,* Vol. 3, No. 6, pp. 95-108, June 2014.

[29] Kalpana Saini, M.L. Dewal and Manojkumar Rohit, "Segmentation of Mitral Regurgitation Jet using the combination of Wavelet and Watershed Transformation' *IEEE 8TH International Colloquium on Signal Processing and its Applications*, pp. 74-79, 2012.

[30] Arun Balodi, M.L Dewal, R. S. Anand and Anurag Rawat, "Texture based classification of severity of the Mitral Regurgitation" *Computers in Biology and Medicine,* pp. 1-18, August 2017.

[31] Kamaljeet Kaur, "Digital Image Processing in Ultrasound Images", *International Journal on Recent and Innovation Trends in Computing and Communication*, Vol 1, No.4 , pp 388-393, March 2013.

[32] James F. Havlice and Jon *C.* Taenzer, "Medical Ultrasonic Imaging: An Overview of Principles and Instrumentation", *Proceedings of the IEEE,* Vol 67, No. 4,pp 620-641, May 1979.

[33] Carovac A, Smajlovic F and Junuzovic D, "Application of Ultrasound in Medicine", *Acta Inform Med*, Vol 19, No.3, pp 168-171, September 2011.

[34] Robert W. Coatney, "Ultrasound Imaging: Principles and Applications in Rodent Research", *ILAR J*, Vol.42, No.3, pp 233-247, March 2001.

[35] I. M. Hellemans, E. G. Pieper, A. C. Ravelli, J. P. Hamer, W. Jaarsma, R. B. van den Brink, C. H. Peels, H. A. van Swieten, J. G. Tijssen, C. A. Visser, et al., "Comparison of transthoracic and transesophageal echocardiography with surgical findings in mitral regurgitation", *The American journal of cardiology*, Vol.77, No.9, pp. 728-733, May 1996.

[36] M. Enriquez-Sarano, W. K. Freeman, C. M. Tribouilloy, T. A. Orszulak, B. K. Khandheria, J. B. Seward, K. R. Bailey, A. J. Tajik, "Functional anatomy of mitral regurgitation: accuracy and outcome implications of transesophageal echocardiography", *Journal of the American College of Cardiology* ,Vol.34, No. 4, pp. 1129-1136, Oct 1999.

[37] H.-D. Cheng, X. H. Jiang, Y. Sun, J. Wang, "Color image segmentation: advances and prospects", *Pattern recognition*, Vol.34, No. 12, pp. 2259-2281, Dec 2001.

[38] N. R. Pal, S. K. Pal, "A review on image segmentation techniques", *Pattern recognition*, Vol.26, No. 9, pp. 1277-1294, Jan 1993.

[39] E. C. Jones, R. B. Devereux, M. J. Roman, J. E. Liu, D. Fishman, E. T. Lee, T. K. Welty, R. R. Fabsitz, B. V. Howard, "Prevalence and correlates of mitral regurgitation in a population-based sample (the strong heart study)", *American Journal of Cardiology*, Vol. 87, No.3, pp. 298-304, Dec 2001.

[40] D. S. Bach, G. M. Deeb, S. F. Bolling, "Accuracy of intraoperative transesophageal echocardiography for estimating the severity of functional mitral regurgitation", *American Journal of Cardiology*, Vol. 76, No.7, pp. 508-512, Oct 1999.

[41] H. Aotsuka, K. Tobita, H. Hamada, M. Uchishiba, S. Tateno, K. Matsuo, T. Fujiwara, K. Niwa,"Validation of the proximal isovelocity surface area method for assessing mitral regurgitation in children", *Pediatric cardiology*, Vol. 17, No. 6, pp.351-359, Feb 1999.

[42] M. Enriquez-Sarano, A.-J. Basmadjian, A. Rossi, K. R. Bailey, J. B. Seward, A. J. Tajik, "Progression of mitral regurgitation: a prospective doppler echocardiographic study", *Journal of the American College of Cardiology*, Vol. 34, No. 4, pp. 1137-1144, May 1996.

[43] W. P. Santamore, F. N. DiMeo, P. R. Lynch, A comparative study of various single-plane cardiographic methods to measure left-ventricular volume, *IEEE Transactions on Biomedical Engineering*, Vol. 6, No.2, pp. 417-421, Sept 1993.

[44] A. H. Torp, S. I. Rabben, A. Stoylen, H. Ihlen, K. Andersen, L.-A. Brodin, J. Olstod, "Automatic detection and tracking of left ventricular landmarks in echocardiography", *Ultrasonics Symposium IEEE*, Vol. 1, pp. 474-477, Feb 1998.

[45] W. Ohyama, T. Wakabayashi, F. Kimura, S. Tsuruoka, K. Sekioka, Automatic left ventricular endocardium detection in echocardiograms based on ternary thresholding method, "*Pattern Recognition IEEE*", Vol. 4, pp. 320-323, Sept.2001.

[46] J. Hansegard, E. Steen, S. I. Rabben, A. H. Torp, H. Torp, S. Frigstad, B. Olstad, Knowledge based extraction of the left ventricular endocardial boundary from 2D echocardiograms, "*Ultrasonics Symposium IEEE*", Vol. 3, pp. 2121-2124, Oct 2004

45